INTERNATIONAL ATOMIC ENERGY AGENCY
UNITED NATIONS EDUCATIONAL, SCIENTIFIC AND CULTURAL ORGANIZATION
INTERNATIONAL CENTRE FOR THEORETICAL PHYSICS
I.C.T.P., P.O. BOX 586, 34100 TRIESTE, ITALY, CABLE CENTRATOM TRIESTE

UNITED NATIONS INDUSTRIAL DEVELOPMENT ORGANIZATION

INTERNATIONAL CENTRE FOR SCIENCE AND HIGH TECHNOLOGY

H4.SMR/544 - 5

Winter College on Ultrafast Phenomena

18 February - 8 March 1991

FEMTOSECOND OPTICS

Z. Bor
Jate University
Department of Optics & Quantumelectronics
Szeged, Hungary

FEMTOSECOND OPTICS

Zsolt BOR

JATE UNIVERSITY
DEPARTMENT OF OPTICS AND QUANTUMELECTRONICS

6720 SZEGED, DOM TER 9, HUNGARY
T: (62) 22529
Fax: (62) 12921

TIME OF FLIGHT INTERFEROMETER

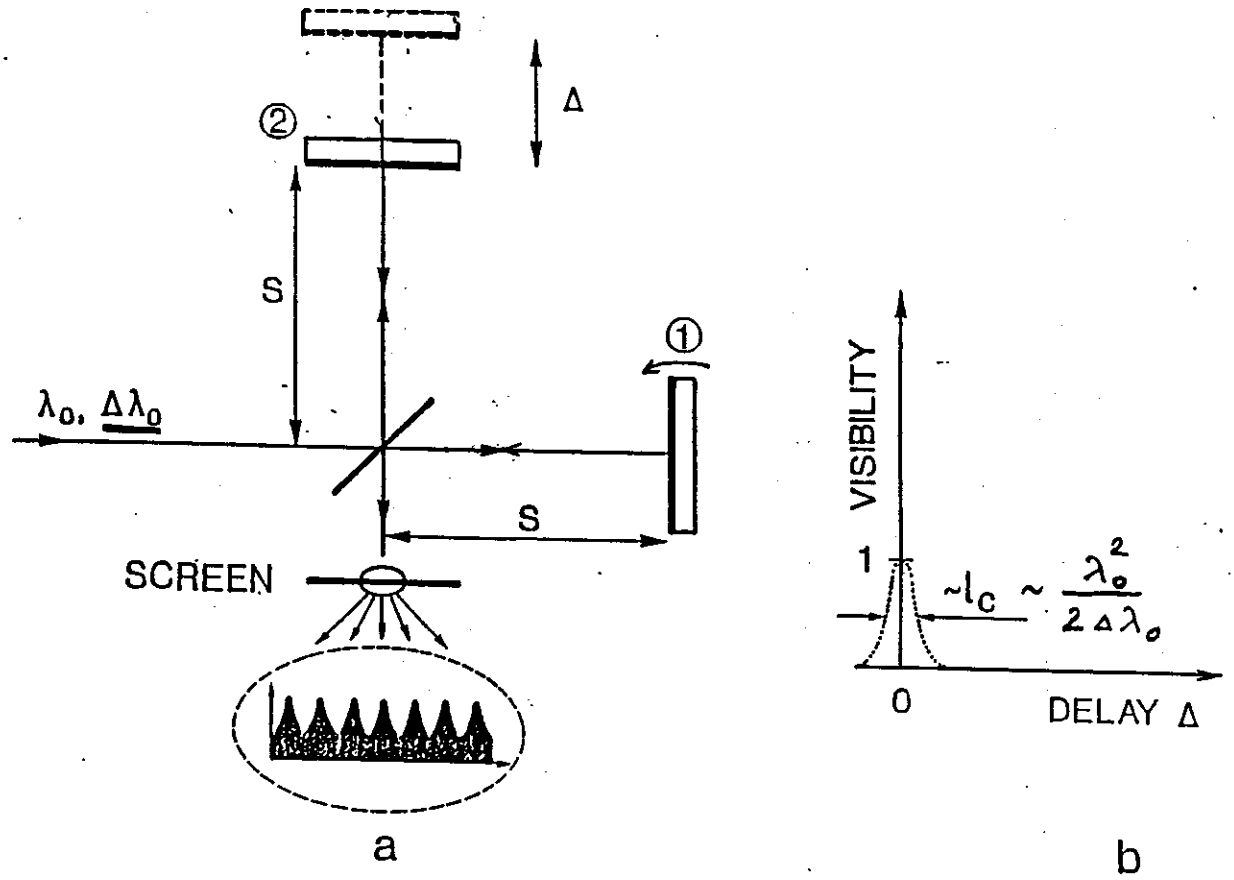

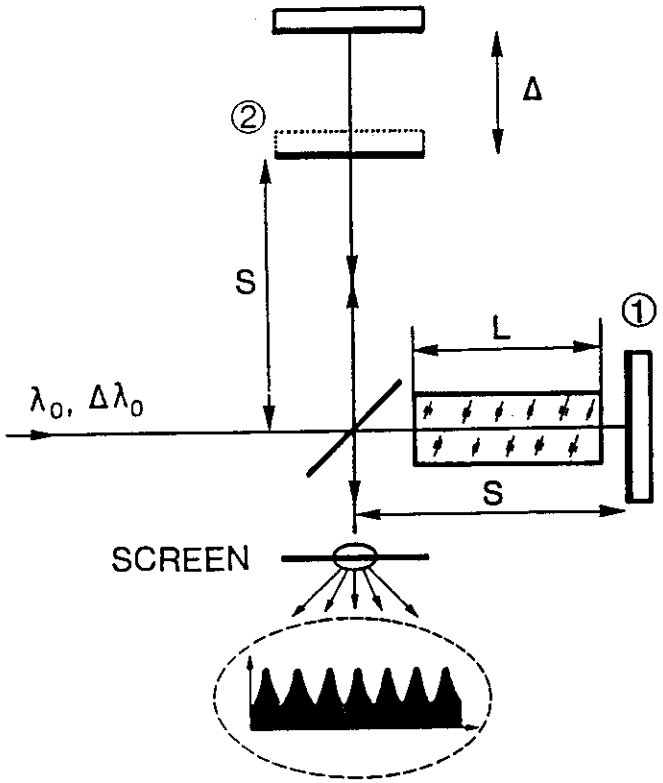

a

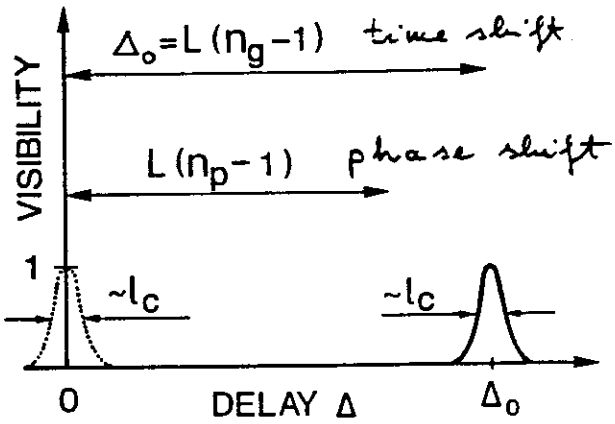

b

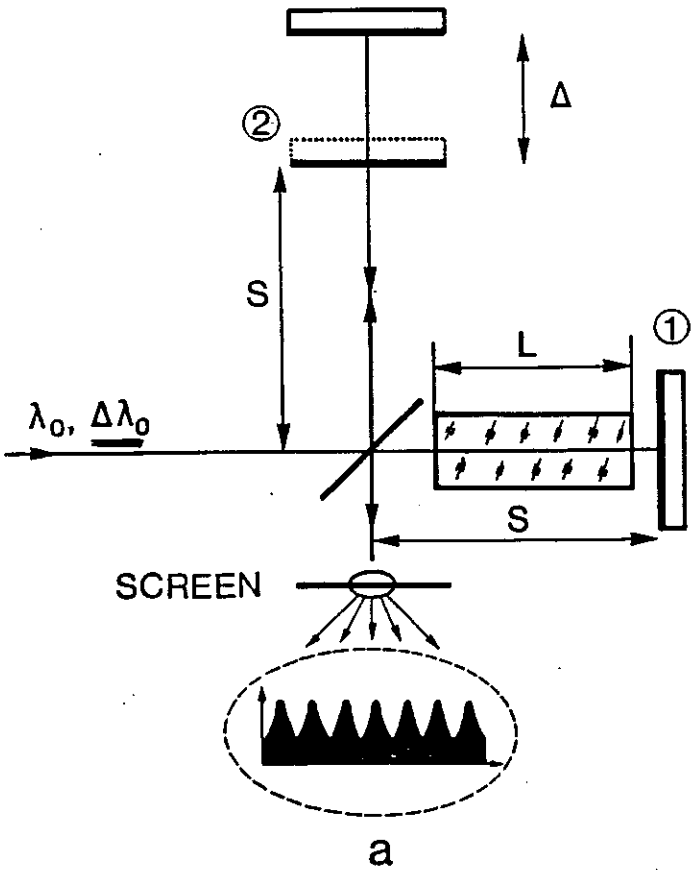

a

$$\varphi_1 = \frac{4\pi}{\lambda_o}\left[(S-L) + L\, n_p(\lambda_o)\right].$$

$$\varphi_2 = \frac{4\pi}{\lambda_o}\left[S + \Delta\right].$$

$$\frac{d}{d\lambda_o}(\varphi_1 - \varphi_2) = 0.$$

$$\Delta_0 = L\left(\underbrace{n_p - \lambda_0 \frac{dn_p}{d\lambda_0}}_{n_g} - 1\right).$$

$$\boxed{\Delta_0 = L(n_g - 1)}$$

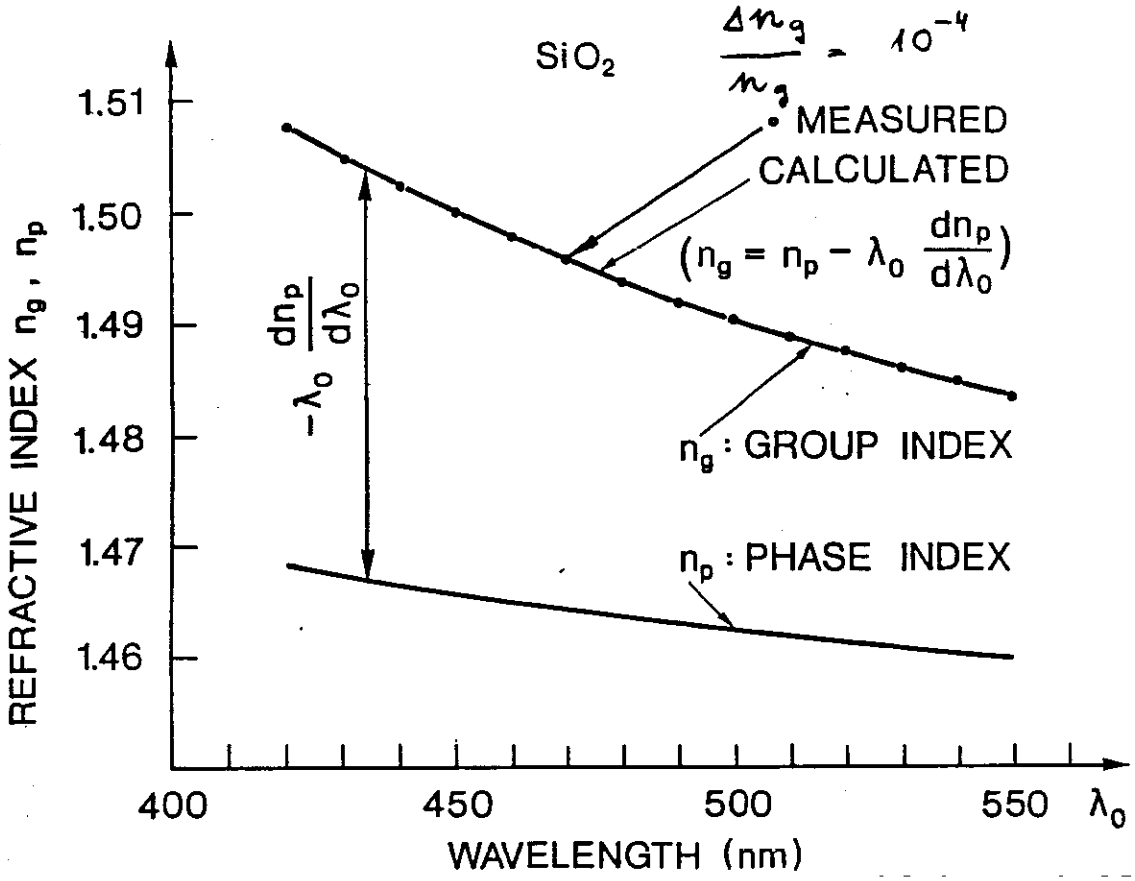

5

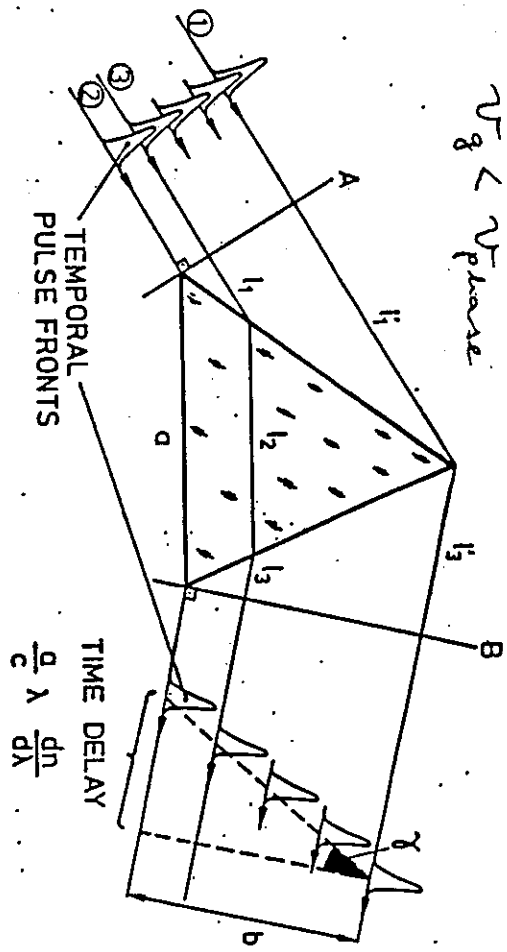

$$\text{tg}\gamma = \frac{a}{b}\lambda\frac{dn}{d\lambda}$$

$$\frac{d\varepsilon}{d\lambda} = \frac{a}{b}\frac{dn}{d\lambda}$$

$$\boxed{\text{tg}\gamma = \lambda\frac{d\varepsilon}{d\lambda}}$$

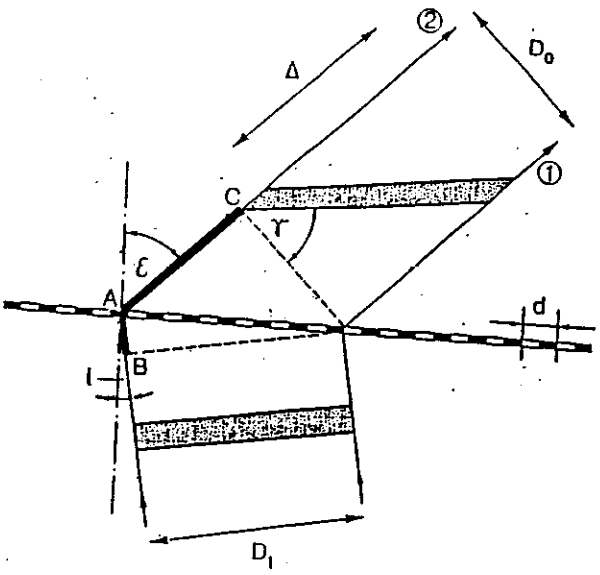

$$\sin i + \sin \varepsilon = k \frac{\lambda}{d}$$

$$\frac{d\varepsilon}{d\lambda} = \frac{k}{d \cos \varepsilon}$$

$$\textcircled{\Delta} = \overline{AC} + \overline{AB} = \frac{D_i}{\cos i} \sin i + \frac{D_0}{\cos \varepsilon} \sin \varepsilon$$

$$\frac{D_i}{\cos i} = \frac{D_0}{\cos \varepsilon}$$

$$tg\gamma = \frac{\Delta}{D_0}$$

$$\boxed{tg\gamma = \lambda \frac{d\varepsilon}{d\lambda}}$$

$$\Delta\varepsilon = 0.886 \frac{\lambda}{D_0}$$

$$\Delta\lambda = \left(\frac{d\varepsilon}{d\lambda}\right)^{-1} \Delta\varepsilon$$

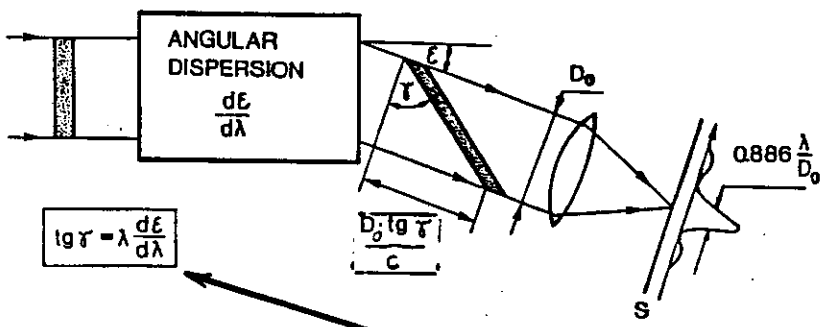

$$\left|\frac{\Delta\nu}{\nu}\right| = \left|\frac{\Delta\lambda}{\lambda}\right|$$

$$\Delta\nu = \frac{0.886}{\frac{D_0}{c} tg\gamma}$$

$$\boxed{\Delta\nu = \frac{0.886}{\Delta\tau}}$$

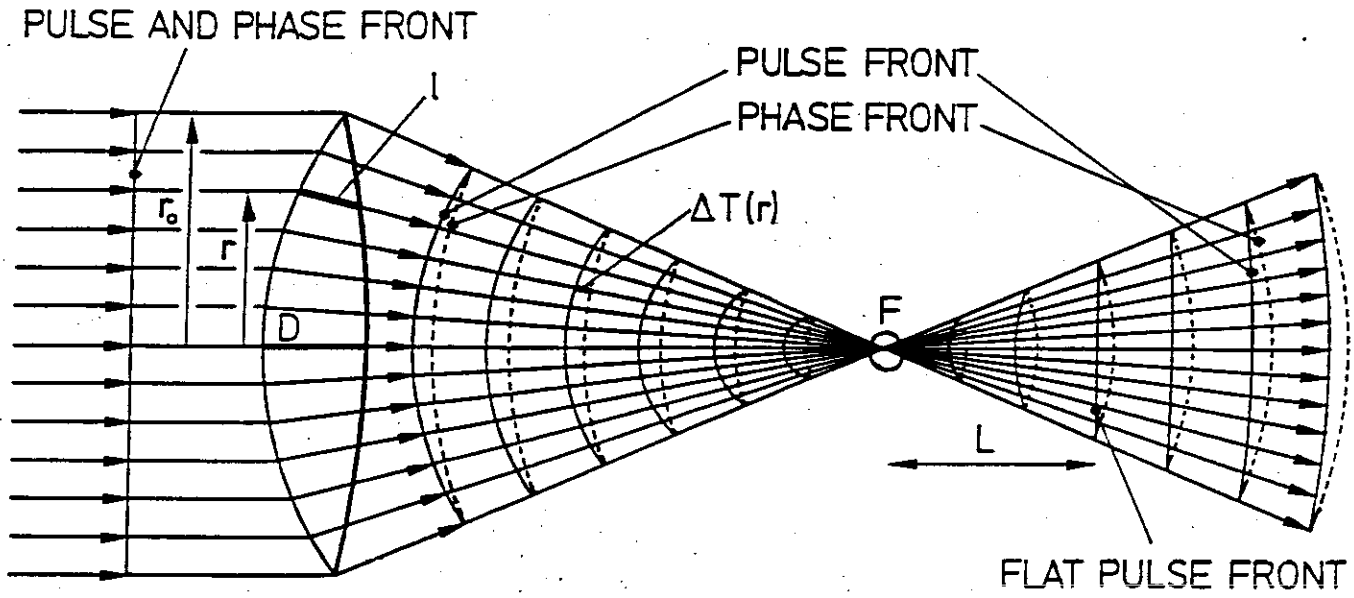

$r_0 = 40$ mm
$f = 150$ mm
$\lambda = 249$ nm
SiO_2

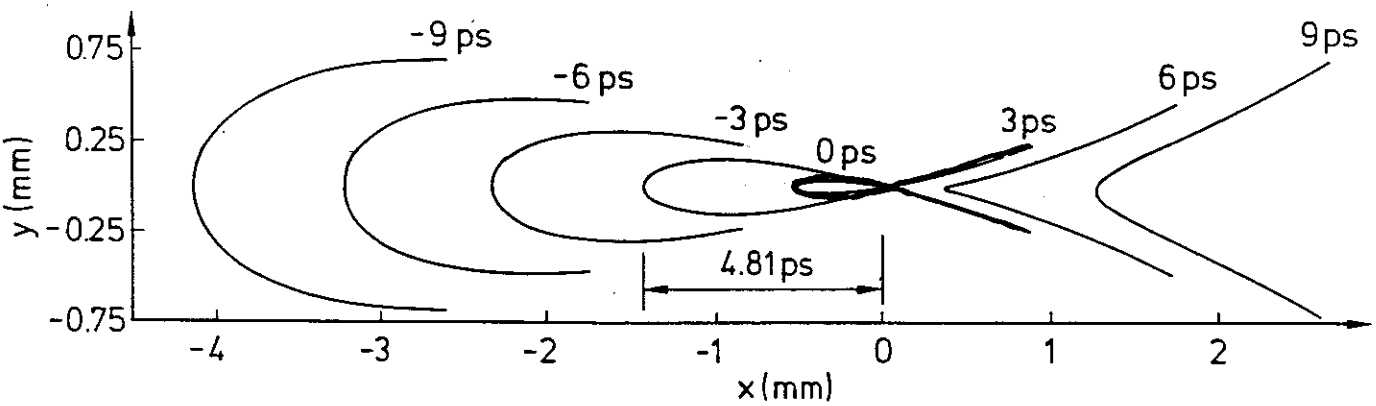

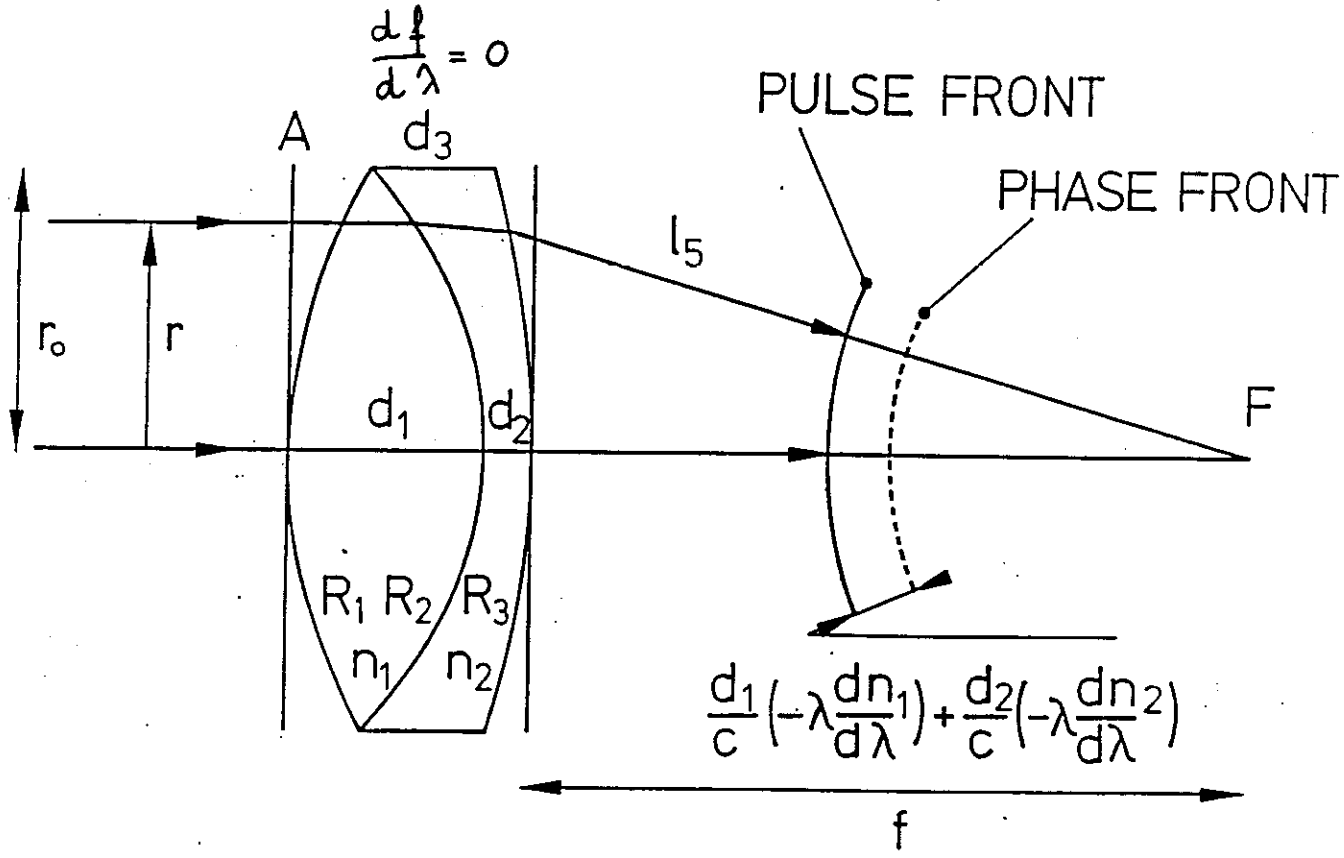

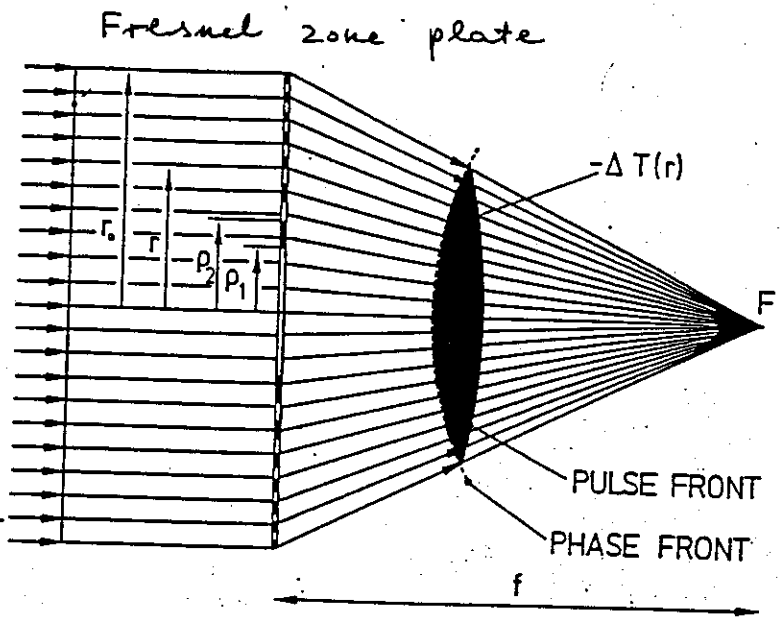

$$\rho_i = \rho_1\sqrt{i}$$

$$f = \rho_1^2/\lambda$$

$$\left.\begin{aligned}\frac{df}{d\lambda} &= -\frac{f}{\lambda}\\ \Delta T(r) &= -\frac{r_0^2 - r^2}{2f\cdot c}\end{aligned}\right\} \quad \Delta T(r) = \frac{r_0^2 - r^2}{2cf^2}\,\lambda\frac{df}{d\lambda}$$

Z. BOR: OPT. LETT. 14 (1989) 119
Z. BOR: J. MOD. OPT. 35 (1988) 1907

General expression

$$\Delta T(r) = \frac{r_0^2 - r^2}{2c\ f^2}\ \lambda\ \frac{df}{d\lambda}$$

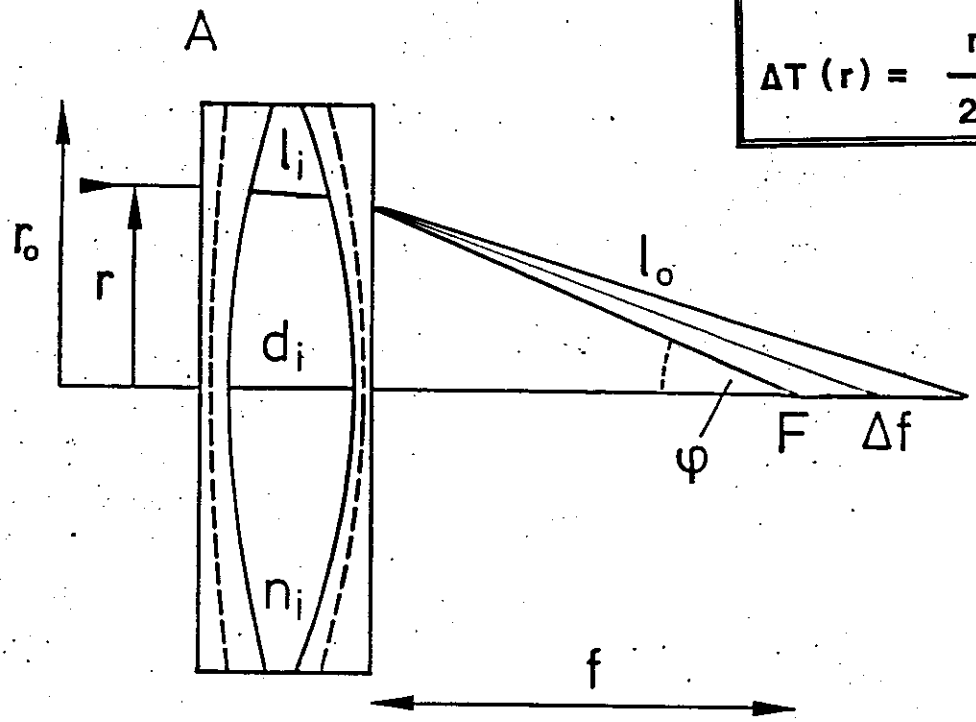

Z. BOR: OPT. LETT. 14 (1989) 119
Z. BOR: J. MOD. OPT. 35 (1988) 1907

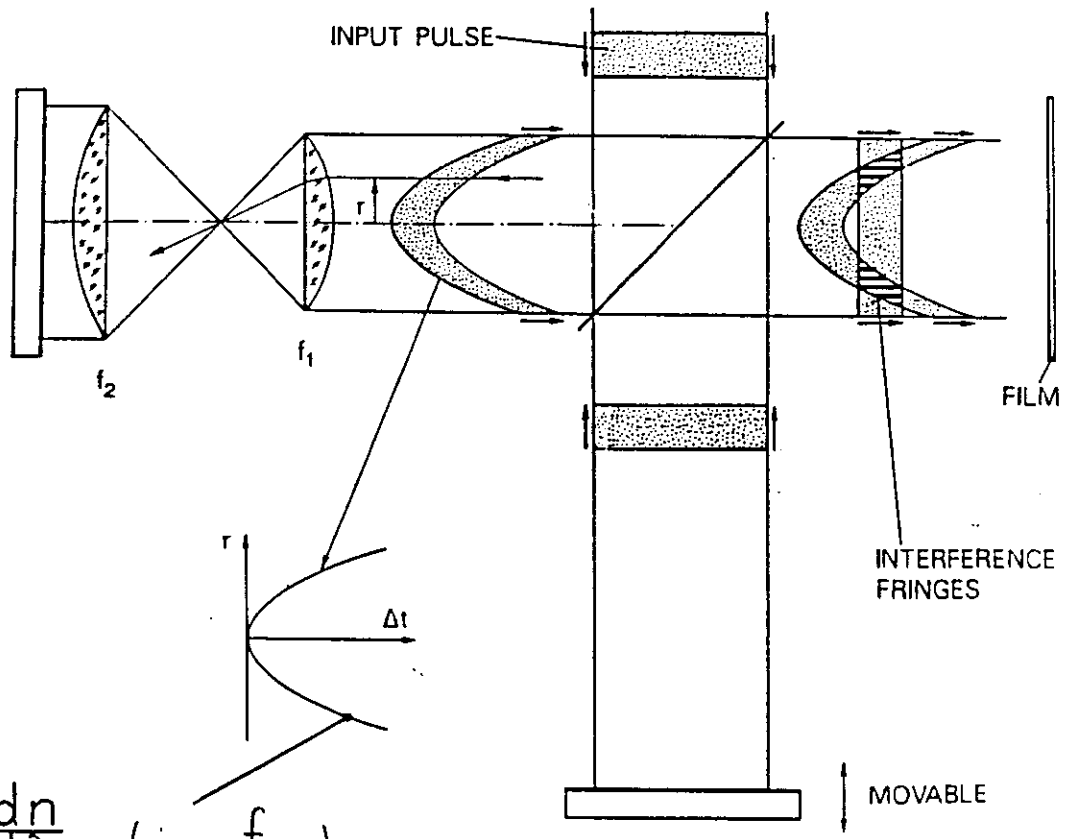

$$\Delta t = \frac{-\lambda \frac{dn}{d\lambda}}{c f_1 (n-1)} \left(1 + \frac{f_2}{f_1}\right) r^2$$

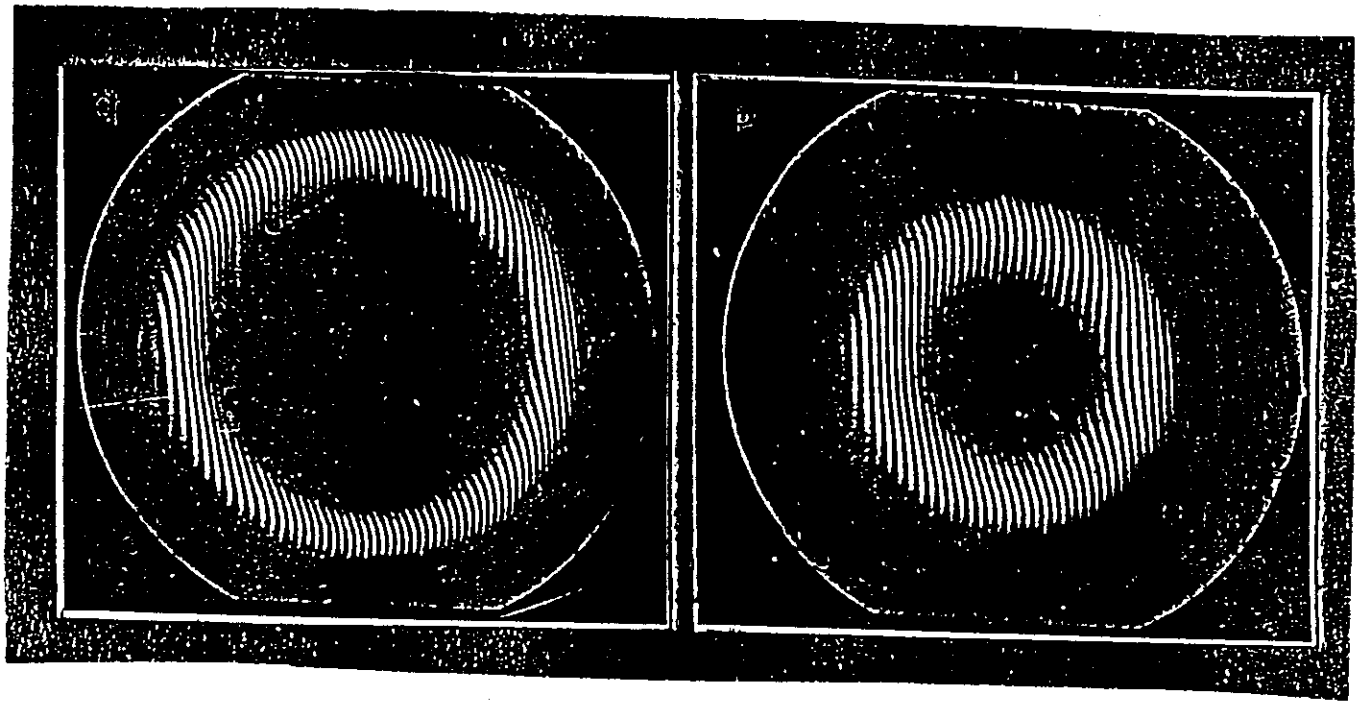

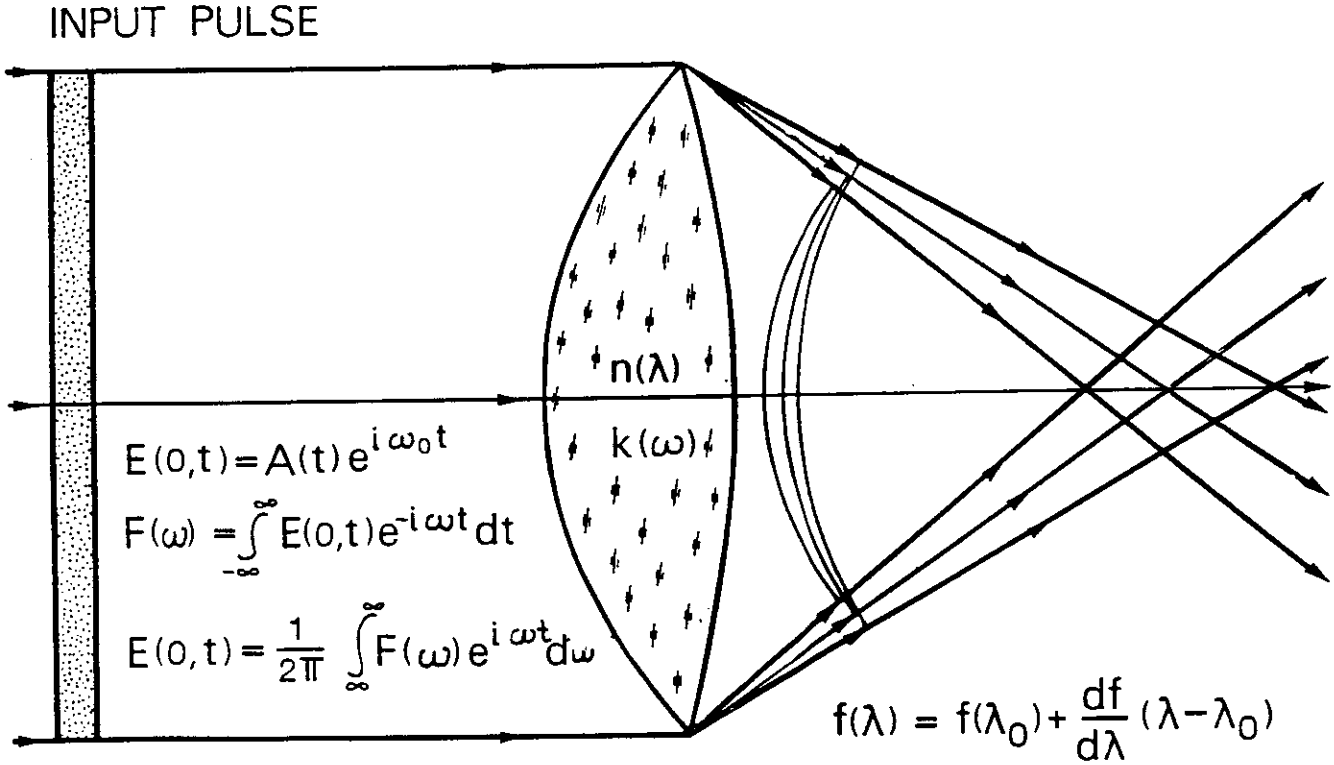
INPUT PULSE
n(λ)
k(ω)
E(0,t)=A(t)e^{iω₀t}
F(ω)=∫_{-∞}^{∞} E(0,t)e^{-iωt}dt
E(0,t)=1/2π ∫_{-∞}^{∞} F(ω)e^{iωt}dω
f(λ) = f(λ₀)+ df/dλ (λ−λ₀)
PLANE WAVES
AIRY-PATTERN
(SPHERICAL WAVES)

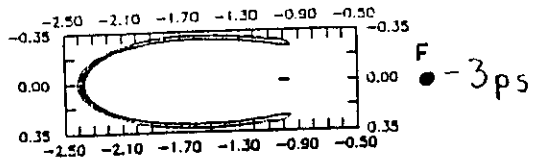
F
-3ps

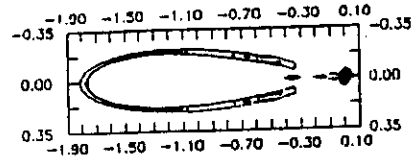
-1ps

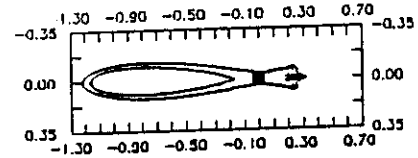
1 ps

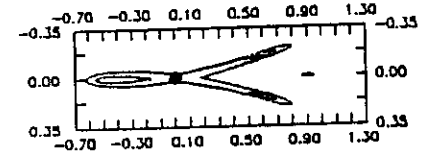
3 ps

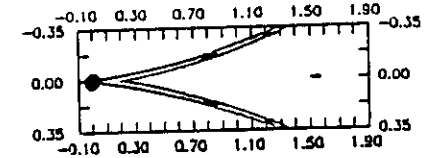
5ps

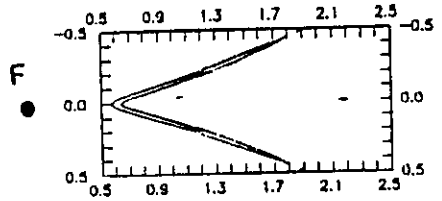
F
7ps

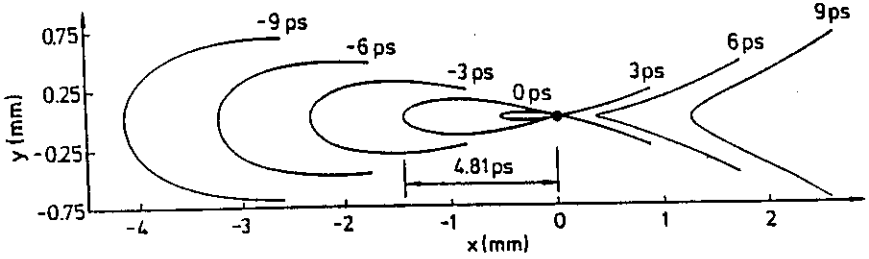
-9 ps
-6 ps
-3 ps
0 ps
3ps
6ps
9ps
4.81ps
y (mm)
x (mm)

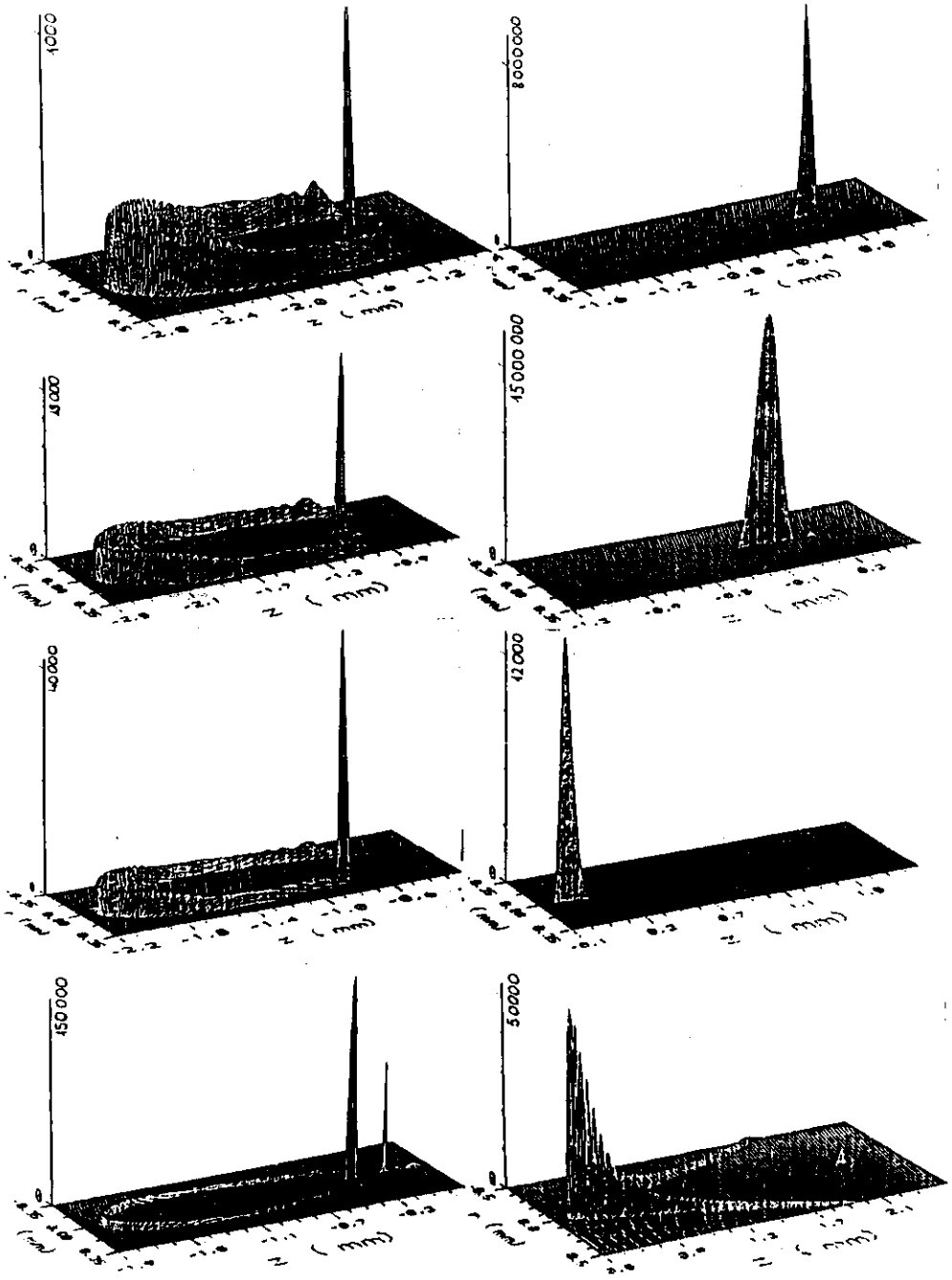

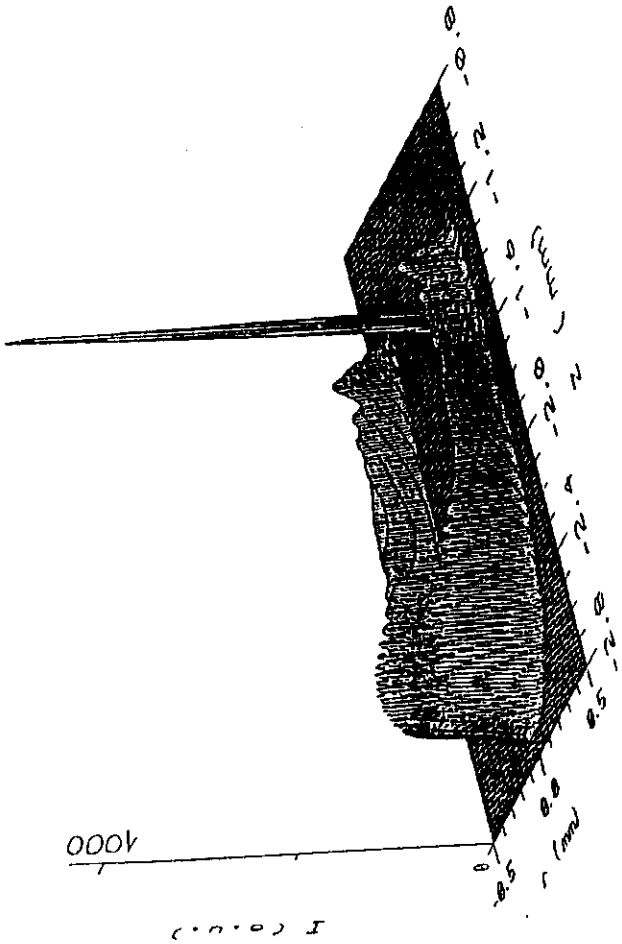

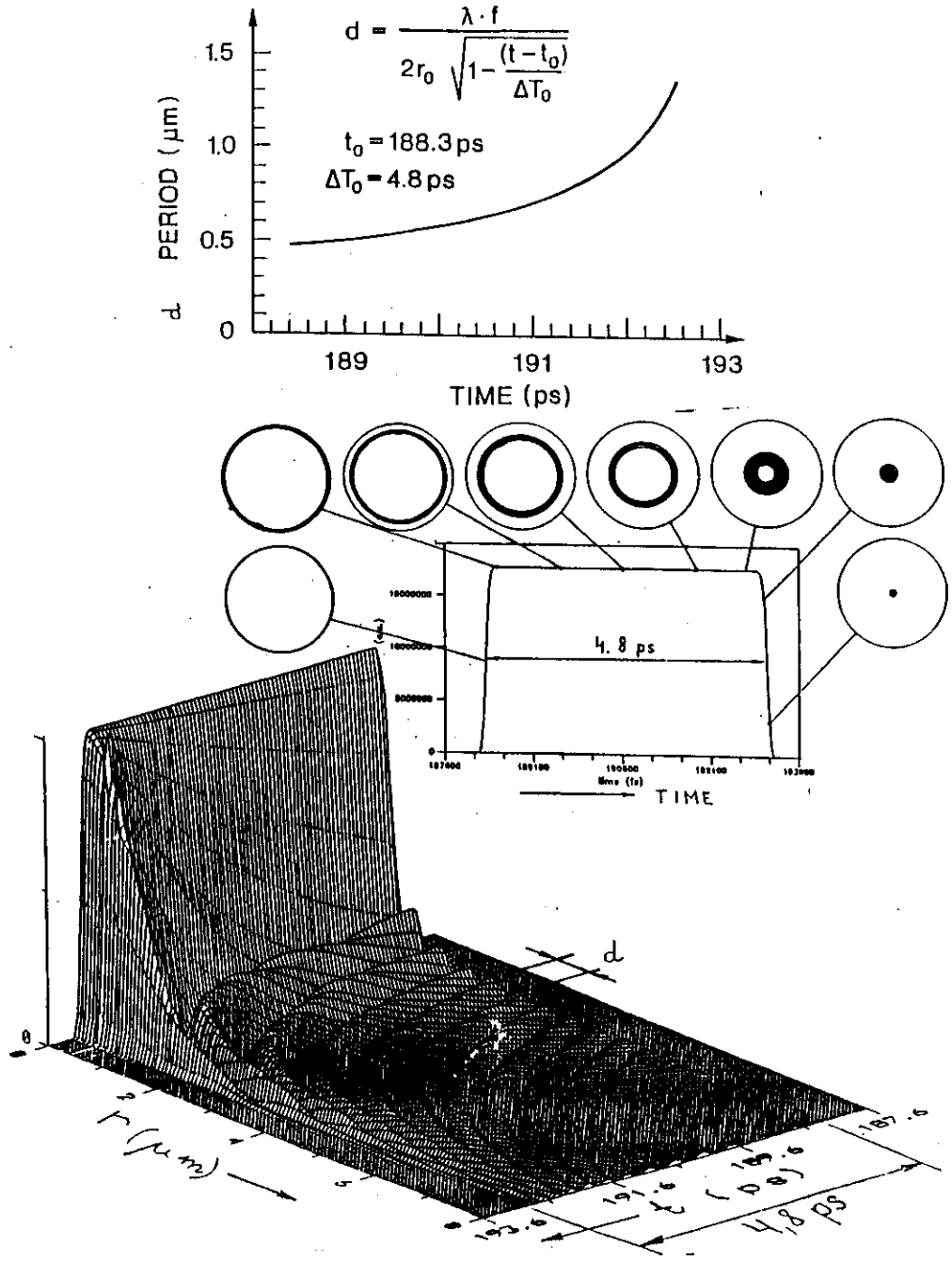
d = λ·f / 2r0 √(1 − (t − t0)/ΔT0)
t0 = 188.3 ps
ΔT0 = 4.8 ps
PERIOD (μm)
d
1.5
1.0
0.5
0
189
191
193
TIME (ps)
4.8 ps
TIME
d
r (μm)
t (ps)
4.8 ps

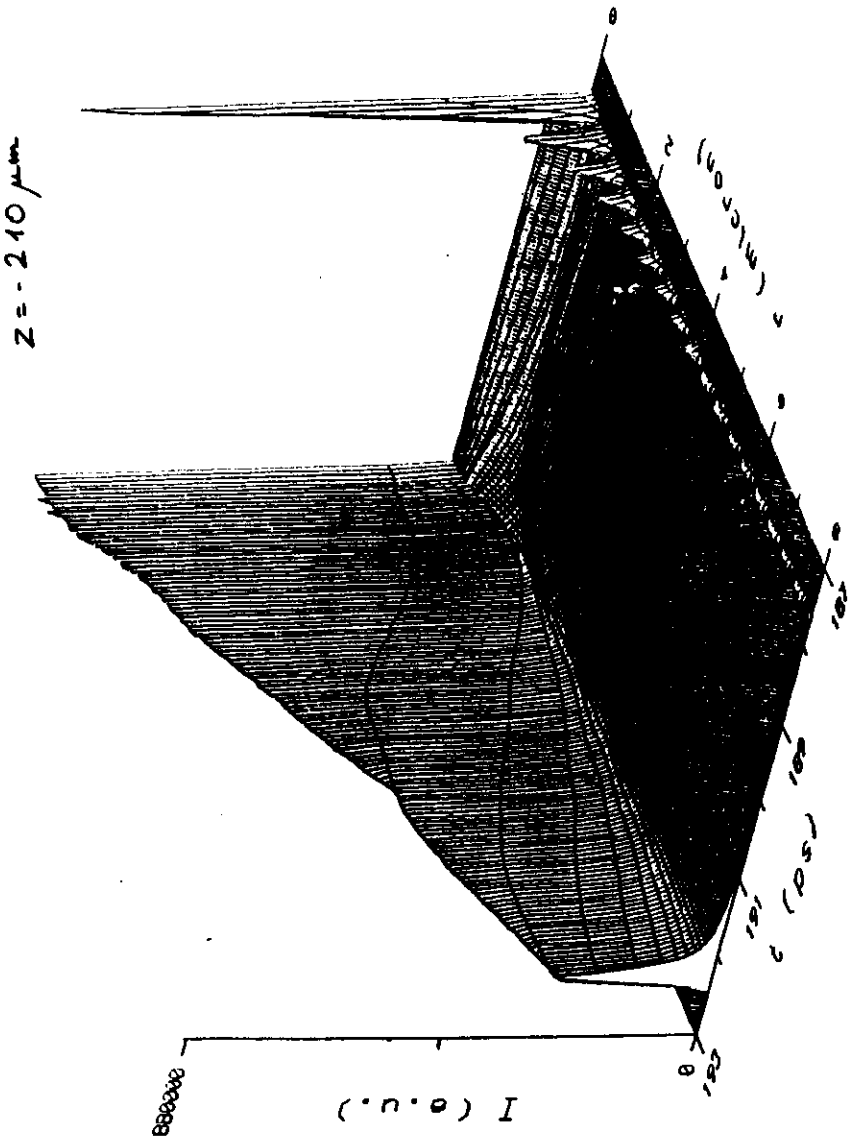

JOURNAL OF MODERN OPTICS, 1988, VOL. 35, NO. 12, 1907–1918

Distortion of femtosecond laser pulses in lenses and lens systems

Z. BOR†

Max-Planck Institut für biophysikalische Chemie,
Abteilung Laserphysik, Postfach 2841,
D-3400 Göttingen, F.R. Germany

Abstract. Owing to the difference between the phase and group velocity, the pulse front may be delayed with respect to the phase front by several picoseconds when traversing a lens or a lens system. The delay is a parabolic function of the input radius. The delay is calculated for singlet lenses, achromats, compound lenses, telescopes. The effect may be two to three orders of magnitude larger than the broadening due to group velocity dispersion in the materials of the lenses.

1. Introduction

The temporal and spatial profile of a femtosecond pulse is strongly affected by the dispersion properties of the optical media. The dispersive properties of prisms have been extensively studied. Prism systems are successfully used for intra- and extra-cavity pulse compression [1–13].

However, very little attention has been paid to propagation effects in lenses, lens systems, telescopes etc. [14–16]. In lenses, two kinds of effect occur. The pulse front, which is defined as the surface coinciding with the peak of the pulse, moves with group velocity and is thus delayed with respect to the phase front. The peculiarity of the lens is that this delay is different for various regions of the lens cross-section. This is due to the fact that the path length of the beam in the media of the lens depends on the input radius r (see figure 1). This effect will be referred to as propagation time difference (PTD). PTD is proportional to $dn/d\lambda$.

The second effect is the pulse broadening due to group velocity dispersion (GVD) of the material of the lens. This effect is proportional to $d^2n/d\lambda^2$ of the materials. Since this broadening is also dependent on the path length in the glass, the broadening is also dependent on r.

The effect of PTD and the broadening due to GVD can be precisely calculated by ray tracing. However, ray tracing requires an *a priori* knowledge of the construction parameters of the lens system. Besides, from the numerical results of ray tracing it is difficult to recognize the physical relationships.

In this paper we derive some equations describing PTD and pulse broadening due to GVD in lenses. Special attention will be paid to singlet lenses, achromats, and telescopes.

† Permanent address: Research Group on Laser Physics of the Hungarian Academy of Sciences, Dóm tér 9, H-6720 Szeged, Hungary.

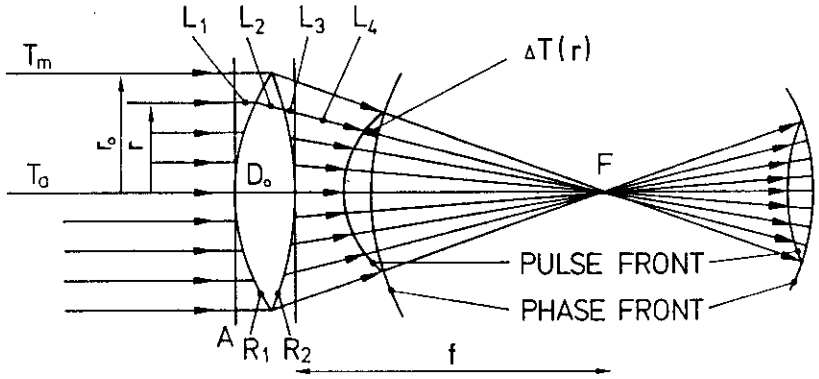

Figure 1. Owing to the difference between the group and phase velocity, the temporal front is delayed with respect to the phase front.

2. Propagation time through a singlet lens

In order to calculate the propagation time we start from Fermat's principle

$$L_1 + nL_2 + L_3 + L_4 = nD_0 + f, \tag{1}$$

where f is the focal length and L_1, L_2, L_3, L_4, D_0 and f are defined in figure 1.

A pulse is propagating in a medium with the group velocity v_g which is calculated as $v_g = d\omega/dk$ [17, 18, 21], where ω is the angular frequency and k is the wave-vector. For solving optical problems, instead of ω and k it is more convenient to use the wavelength in vacuum λ and the refractive index $n(\lambda)$. Then the group velocity is expressed as $v_g = c/(n - \lambda\, dn/d\lambda)$ [1, 3, 18]. It is worth noting that in some textbooks [19, 20, 21] v_g is given by an expression $v_g = c[1 + \lambda/(n\, dn/d\lambda)]/n$ without stating clearly that here λ means the wavelength in the medium and not in vacuum. Therefore this second expression is less useful than the first one, because the refractive index is tabulated or approximated by polynomials for the vacuum wavelength and not for the wavelength in medium [22–24]. Throughout this paper we use the first expression with λ being the wavelength in vacuum.

The propagation time $T(r)$ of a plane wave from plane A to the focal point F (see figure 1) can be calculated as

$$T(r) = \frac{L_1 + L_3 + L_4}{c} + \frac{L_2}{c}\left(n - \lambda\frac{dn}{d\lambda}\right). \tag{2}$$

In the paraxial approximation [17] we obtain for D_0, L_2, and f (see figure 1)

$$D_0 = \frac{r_0^2}{2}\left(\frac{1}{R_1} + \frac{1}{R_2}\right), \tag{3}$$

$$L_2 = \frac{r_0^2 - r^2}{2}\left(\frac{1}{R_1} + \frac{1}{R_2}\right), \tag{4}$$

$$\frac{1}{f} = (n-1)\left(\frac{1}{R_1} + \frac{1}{R_2}\right), \tag{5}$$

where r and r_0 are the input radii of an arbitrary and the marginal ray respectively, and R_1 and R_2 are the radii of curvature of the lens surfaces.

Using (1) (5) and rearranging we finally obtain the propagation time

$$T(r) = \frac{f}{c} + \frac{D_0}{c}\left(n - \lambda\frac{dn}{d\lambda}\right) + \frac{r^2}{2c}\left(\frac{1}{R_1} + \frac{1}{R_2}\right)\lambda\frac{dn}{d\lambda}. \tag{6}$$

Substituting (3) into (6) and taking $r = r_0$ we obtain the propagation time for the marginal ray

$$T_m \equiv T(r = r_0) = \frac{f}{c} + \frac{D_0 n}{c}. \tag{7}$$

Since the optical path from plane A to F is $nD_0 + f$ (see figure 1) it follows that the marginal ray propagates with the phase velocity.

The temporal delay $\Delta T(r)$ between the phase front and the pulse front for a ray at an arbitrary input radius r is

$$\Delta T(r) \equiv T(r) - T_m = \frac{r_0^2 - r^2}{2c}\left(\frac{1}{R_1} + \frac{1}{R_2}\right)\left(-\lambda\frac{dn}{d\lambda}\right), \tag{8}$$

or by using (5)

$$\Delta T(r) = \frac{r_0^2 - r^2}{2cf(n-1)}\left(-\lambda\frac{dn}{d\lambda}\right). \tag{9}$$

For optical materials of practical interest, $\lambda\, dn/d\lambda$ has a negative value in the spectral range of transparency. The axial part of the beam is, therefore, delayed with respect to the marginal part.

The effect of PTD is illustrated in figure 2 and figure 3, which show the locations of the pulse fronts at different moments. The equations describing the pulse fronts are

$$x = c(t - \Delta T(r))\cos\alpha, \tag{10}$$

$$y = c(t - T(r))\sin\alpha, \tag{11}$$

where x and y are the spatial coordinates measured from the focal point, $\alpha = \text{arctg}\,(r/f)$ and the origin of time t is chosen so that the marginal ray propagating with phase velocity arrives at the focus at $t = 0$.

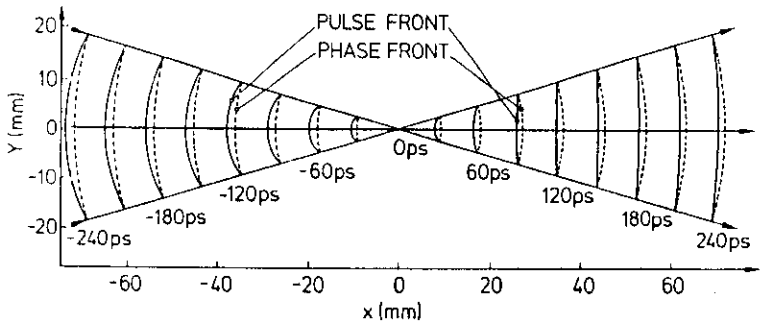

Figure 2. Behaviour of the pulse and phase fronts behind a lens. Notice that around $x = 40$ mm the pulse front changes from convex to concave.

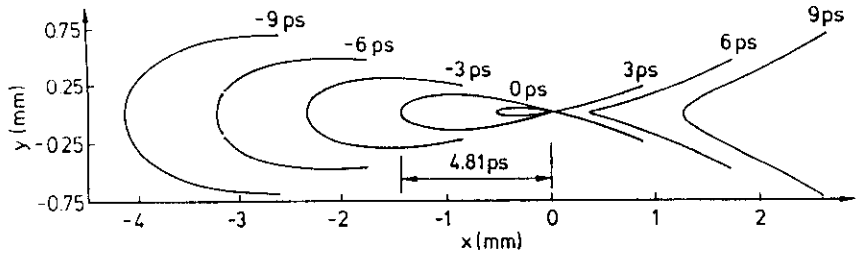

Figure 3. Behaviour of the pulse and phase front in the vicinity of the focal plane (geometrical optical approximation). The temporal delay between the marginal and axial ray is 4·81 ps. The formation of the loop means that for $0<t<4{\cdot}81$ ps the pulse propagating along the marginal ray has passed the focus, while the axial part has not reached it.

Figure 2 shows the pulse and phase fronts for a fused silica lens having $f=150$ mm, $r_0=40$ mm, $n=1{\cdot}50799$ [23], $\lambda\, dn/d\lambda=-0{\cdot}1375$ at the wavelength of the KrF excimer laser (249 nm).

The shape of the pulse front near to the focal region is shown in figure 3. A peculiar feature is the formation of a loop for times $0<t<\Delta T(r_0)$. The reason for this is that for $0<t<\Delta T(r_0)$ the part of the pulse propagating marginally has already passed through the focal point F, while the axially propagating part has not reached it yet. The present analysis makes use of the geometrical optical approximation. It is, therefore, not valid in the proximity (about a few hundred micrometres) of the focus. In this range the shape of the pulse front may be calculated by solving the Kirchhoff–Fresnel integrals. Such calculations have been carried out previously by Martinez [5] for a much simpler case (i.e. for plane waves tilted by gratings or prisms).

Figures 2 and 3 demonstrate clearly the importance of PTD for ultrashort pulses. A photodetector located at the Gaussian plane of the lens would detect a signal stretched by $T(r=0)-T(r=r_0)$ which amounts to 4·81 ps for the lens specified above.

It is interesting to note that the curvature of the pulse front changes from convex to concave behind the focus around $x=40$ mm (figure 2). From simple geometrical consideration it can be shown that at

$$L=\frac{f}{(n-1)}\left(-\lambda\frac{dn}{d\lambda}\right) \tag{12}$$

the pulse front is flat, while the phase front is a sphere having a radius of L. This property of the lens can be used to avoid the unwanted effect of the radius dependent propagation time $T(r)$. For a silica lens at 249 nm this distance is at $L=0{\cdot}27f$ behind the focus F.

The pulse front may be also affected by the spherical aberration of the lens. The study of this effect is beyond the scope of this paper. It is worth noting that Fermat's principle (1) implicitly assumes that the spherical aberration is neglected.

3. Propagation time through an achromatic doublet

The derivation of the propagation time for an achromatic doublet runs analogously to the one given above for the singlet lens. Fermat's principle for an achromat is described as

$$l_1+n_1l_2+n_2l_3+l_4+l_5=d_1n_1+d_2n_2+f. \tag{13}$$

The propagation time from plane A to the focal point F can be calculated as

$$T(r)=\frac{l_1+l_4+l_5}{c}+\frac{l_2}{c}\left(n_1-\lambda\frac{dn_1}{d\lambda}\right)+\frac{l_3}{c}\left(n_2-\lambda\frac{dn_2}{d\lambda}\right). \tag{14}$$

In the paraxial approximation we have

$$l_2=d_1-\frac{r_0^2}{2}\left(\frac{1}{R_1}+\frac{1}{R_2}\right), \tag{15}$$

$$l_3=d_2-\frac{r^2}{2}\left(\frac{1}{R_3}-\frac{1}{R_2}\right), \tag{16}$$

$$d_3=d_2-\frac{r_0^2}{2}\left(\frac{1}{R_3}-\frac{1}{R_2}\right), \tag{17}$$

$$d_1=\frac{r_0^2}{2}\left(\frac{1}{R_1}+\frac{1}{R_2}\right), \tag{18}$$

$$\frac{1}{f}=(n_1-1)\left(\frac{1}{R_1}+\frac{1}{R_2}\right)+(n_2-1)\left(\frac{1}{R_3}-\frac{1}{R_2}\right), \tag{19}$$

where the meaning of the symbols is shown in figure 4.

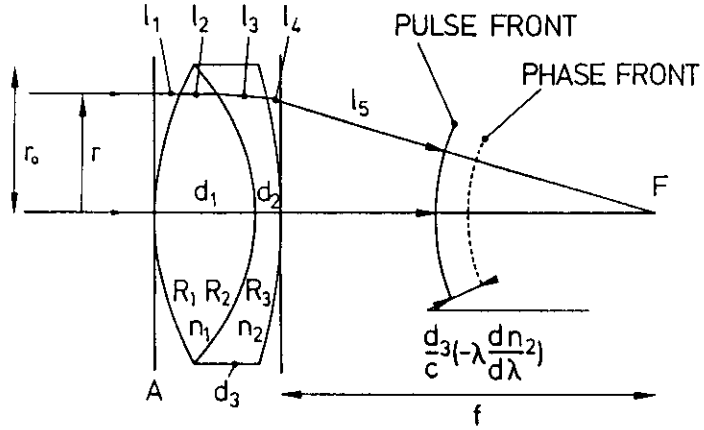

Figure 4. For an achromat the delay between the phase and pulse front is constant across the cross-section of the lens.

From (13) (19) for $T(r)$ we obtain

$$T(r)=\frac{d_1}{c}\left(n_1-\lambda\frac{dn_1}{d\lambda}\right)+\frac{d_2}{c}\left(n_2-\lambda\frac{dn_2}{d\lambda}\right)+\frac{f}{c}+\frac{r}{2c}\left[\left(\frac{1}{R_1}+\frac{1}{R_2}\right)\lambda\frac{dn_1}{d\lambda}+\left(\frac{1}{R_3}-\frac{1}{R_2}\right)\lambda\frac{dn_2}{d\lambda}\right]. \quad (20)$$

If the lens is achromatic at the wavelength of the input beam, then $d(1/f)/d\lambda=0$. Differentiating (19) over the condition of achromatism is expressed as

$$\left(\frac{1}{R_1}+\frac{1}{R_2}\right)\frac{dn_1}{d\lambda}+\left(\frac{1}{R_3}-\frac{1}{R_2}\right)\frac{dn_2}{d\lambda}=0. \quad (21)$$

Therefore, the last term in (20) vanishes, thus

$$T=\frac{d_1}{c}\left(n_1-\lambda\frac{dn_1}{d\lambda}\right)+\frac{d_2}{c}\left(n_2-\lambda\frac{dn_2}{d\lambda}\right)+\frac{f}{c}. \quad (22)$$

From (22) it follows that for an achromat, the delay between the phase and the temporal front is constant over the lens cross-section (figure 4) and is given by $d_1/c(-\lambda\,dn_1/d\lambda)+d_2/c(-\lambda\,dn_2/d\lambda)$. Using (17), (18) and (21) it is easy to show that this delay can be also expressed as $d_3/c(-\lambda\,dn_2/d\lambda)$.

In some experiments the constant delay is not disturbing and so in these cases the use of an achromat instead of a singlet is preferable.

4. Pulse broadening in a singlet lens due to group velocity dispersion

The dependence of v_g on wavelength, which is called group velocity dispersion (GVD), causes a broadening of the pulse. The broadening of an unchirped input pulse due to GVD can be calculated as [18]:

$$\Delta\tau(r)=\frac{\lambda}{c}\frac{d^2n}{d\lambda^2}L_2\Delta\lambda, \quad (23)$$

where L_2 is the light path in the medium. For the case of the lens shown in figure 1 L_2 is given by (4).

It is convenient to express the bandwidth of the pulse $\Delta\lambda$ as

$$\Delta\lambda=\frac{\lambda}{2N}. \quad (24)$$

Here N can be regarded as the number of coherent optical cycles in the pulse. For a transform-limited pulse we have $N=c\tau_p/\lambda$, where τ_p is the pulse duration. The last expression is accurate with the precision of a form factor of the pulse which does not differ considerably from unity.

From (23), (24) and (4) we obtain that the radius-dependent pulse broadening due to GVD is

$$\Delta\tau(r)=\frac{\lambda^2}{2cN}\frac{r_0^2-r^2}{2}\left(\frac{1}{R_1}+\frac{1}{R_2}\right)\frac{d^2n}{d\lambda^2}. \quad (25)$$

Since both effects (PTD and pulse broadening due to GVD) occur simultaneously at the focal point of the lens, it is important to know the ratio of these two effects. From (8) and (25) we obtain

$$\frac{\Delta\tau(r)}{\Delta T(r)}=\frac{A}{2N}. \quad (26)$$

It is worth noting that this ratio is independent of the input radius. In the derivation of (26) the proportionality between the second and the first derivative of the refractive index was used [26]:

$$\lambda\frac{d^2n}{d\lambda^2}=-A\frac{dn}{d\lambda}, \quad (27)$$

where A is a slightly wavelength dependent quantity having a typical value between 2·6 and 4. Higher values of A correspond to the short wavelength spectral cut-off (for details see [26]). Equation (27) is valid for all optical materials of practical interest in the spectral range where they are transparent.

Assuming, for example, a 100 fs long pulse at 249 nm, the number of optical cycles is $N=120$. For fused silica at this wavelength, $\lambda\,dn/d\lambda=-0{\cdot}1375$, and $\lambda\,d^2n/d\lambda^2=2{\cdot}085\,\mu m^{-1}$, resulting in $A=3{\cdot}775$. (The refractive index and its derivatives have been calculated from the polynomial given in [23].) Using the above data we obtain that $\Delta\tau(r)/\Delta T(r)=0{\cdot}0157$, i.e. the effect of propagation time difference $\Delta T(r)$ for suprasil in a singlet lens is nearly two orders of magnitude larger than the pulse broadening due to GVD. For longer pulses when N is higher the ratio (26) is even smaller.

It is worth noting that GVD effects have often been taken into account in experiments. PTD, however, which may be 100–10 000 times larger than pulse broadening due to GVD for pulses of 10–0·1 ps duration, has been neglected or has escaped the attention of experimenters.

5. Pulse broadening in an achromatic doublet due to group velocity dispersion

As we have shown above, for an achromat the propagation time $T(r)$ is constant over the lens cross-section (22), it is, however, wavelength dependent. Staerk *et al.* measured the propagation of short pulses through various streak camera lenses (HAMAMATSU, IMACON and PICI-V) and found that the propagation time can decrease by 37 ps when the wavelength is increased from 351 nm to 527 nm [14, 15]. Such dependence may then cause large errors, experimental artefacts [14, 15] and may result in considerable pulse broadening.

The broadening of the pulse due to GVD observed in the focal plane of an achromatic doublet can be calculated as

$$\Delta\tau(r)=\frac{dT}{d\lambda}\Delta\lambda, \quad (28)$$

where $T(r)$ is given by (22) and $\Delta\lambda$ by (24). Remembering that for an achromat $df/d\lambda=0$, taking the derivative of (22) and using (24) and (28) we obtain

$$\Delta\tau(r)=\frac{\lambda^2}{2cN}\left(d_1\frac{d^2n_1}{d\lambda^2}+d_2\frac{d^2n_2}{d\lambda^2}\right). \quad (29)$$

Thus, an achromat has not only the valuable property that the propagation time is equal for any input radius r (22), but also that pulse broadening caused by the GVD is uniform across the whole beam. This is important, because such broadening which is homogeneous over the beam cross-section can be compensated by grating [25] or prism compressors [2, 3, 7, 8] or in streak camera measurements it can be taken into account by deconvolution [14, 15].

6. Propagation time through a lens system having chromatic aberration

Manufacturers of lenses usually do not specify the radii of curvature, thicknesses and materials of their compound lenses, therefore calculation of pulse broadening due to PTD and GVD either by ray tracing or by using equations (8), (9), (22), (25), (29) is impossible. But since manufacturers do specify the focal length of a lens at several wavelengths, the longitudinal chromatic aberration defined as $\mathrm{d}f/\mathrm{d}\lambda$ can be calculated. Below, we derive the expressions for propagation time $T(r)$ and pulse broadening in which the longitudinal chromatic aberration is used in place of the derivatives of the refractive indices and radii of curvature. The expressions given below are valid for singlet lenses, for achromats and for compound lenses which are chromatically not perfectly compensated at the wavelength of use.

Fermat's principle for a lens consisting of k layers is

$$\sum_1^k n_i(\lambda) l_i(\lambda, r) + l_0(r, \lambda) = \sum_1^k n_i(\lambda) d_i + f, \tag{30}$$

where n_i is the refractive index of the ith layer, $l_i(\lambda, r)$ the path length of the ray in the ith layer, d_i is the path length of the axial ray in the ith layer, l_0, f and φ are shown in figure 5, Δf and Δl_0 are the changes of f and l_0 when the incident wavelength changes from λ to $\lambda + \Delta\lambda$.

The propagation time for a ray with input radius r is

$$T(r) = \sum_1^k \frac{l_i}{c}(\lambda, r)\left[n_i(\lambda) - \lambda \frac{\mathrm{d}n_i(\lambda)}{\mathrm{d}\lambda}\right] + \frac{l_0(r, \lambda)}{c}. \tag{31}$$

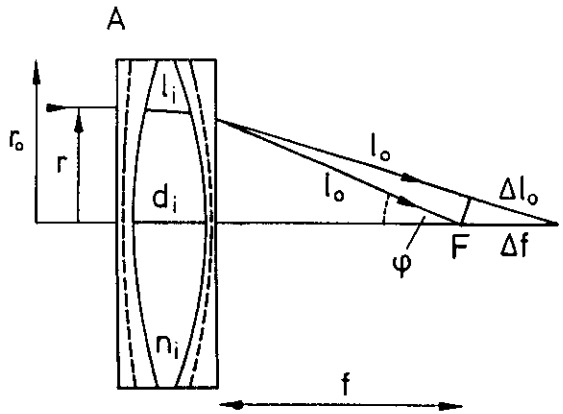

Figure 5. Cross-section through a composite lens.

Taking the derivative of (30) with respect to λ we obtain

$$\sum_1^k l_i(\lambda, r) \frac{\mathrm{d}n_i(\lambda)}{\mathrm{d}\lambda} + \sum_1^k n_i(\lambda) \frac{\mathrm{d}l_i(\lambda, r)}{\mathrm{d}\lambda} + \frac{\mathrm{d}l_0(r, \lambda)}{\mathrm{d}\lambda} = \sum_1^k d_i \frac{\mathrm{d}n_i(\lambda)}{\mathrm{d}\lambda} + \frac{\mathrm{d}f}{\mathrm{d}\lambda}, \tag{32}$$

where $\mathrm{d}f/\mathrm{d}\lambda$ is the longitudinal chromatic aberration of the lens.

In the paraxial approximation, for a thin lens the changes of l_i inside the lens upon a change of the wavelength are small compared with the change of l_0 and, therefore, the approximation

$$\sum_1^k n_i(\lambda) \frac{\mathrm{d}l_i(\lambda, r)}{\mathrm{d}\lambda} = 0 \tag{33}$$

may be used.

From (30)–(33) we obtain

$$T(r) = \sum_1^k \frac{d_i}{c}\left(n_i(\lambda) - \lambda \frac{\mathrm{d}n_i(\lambda)}{\mathrm{d}\lambda}\right) + \frac{f}{c} - \frac{\lambda}{c}\frac{\mathrm{d}f}{\mathrm{d}\lambda}\left(1 - \frac{\mathrm{d}l_0/\mathrm{d}\lambda}{\mathrm{d}f/\mathrm{d}\lambda}\right). \tag{34}$$

From figure 5 we see that

$$\frac{\mathrm{d}l_0/\mathrm{d}\lambda}{\mathrm{d}f/\mathrm{d}\lambda} \approx \frac{\Delta l_0}{\Delta f} = \cos\varphi. \tag{35}$$

Replacing $1 - \cos\varphi$ by $r^2/(2f^2)$ from (35) we see that the radius-dependent delay defined as $\Delta T(r) \equiv T(r) - T(r = r_0)$ can be expressed as

$$\Delta T(r) = \frac{r_0^2 - r^2}{2cf^2} \lambda \frac{\mathrm{d}f}{\mathrm{d}\lambda}. \tag{36}$$

Equation (36) is a very practical expression because it uses the longitudinal chromatic aberration instead of the dispersion of refractive indices. It is also of general validity. Moreover, it can be shown that (36) is also valid for a Fresnel-type focusing zone plate [27] where the time delay between the pulse and phase front is caused by diffraction and not by the difference between the phase and group velocities. Besides that, it can be shown that (36) is the consequence of the uncertainty principle [27].

From (36) it follows that for an achromat (i.e. $df/\mathrm{d}\lambda = 0$), the radius dependent part of the propagation time is 0. This result is identical to the one obtained in (22).

Taking the derivative of (5) with respect to λ yields the longitudinal chromatic aberration of a singlet lens

$$\frac{\mathrm{d}f}{\mathrm{d}\lambda} = -\frac{f}{n-1}\frac{\mathrm{d}n}{\mathrm{d}\lambda}. \tag{37}$$

Inserting (37) to (36), we obtain again (9), as expected.

Just as in the case of a singlet lens, the pulse front will be flat at a distance L behind the Gaussian focal plane [see figure 2 and equation (12)]. Using elementary geometrical considerations together with (36) we arrive at a simple expression

$$L = \lambda \frac{\mathrm{d}f}{\mathrm{d}\lambda}. \tag{38}$$

This expression is in full agreement with (12) and (37) as obtained for a singlet lens.

7. Pulse broadening in a lens system having chromatic aberration

The broadening of the pulse in a lens system can be approximated by

$$\Delta\tau(r)=\sum_1^k \frac{\lambda}{c} l_i \frac{\mathrm{d}^2 n_i}{\mathrm{d}\lambda^2}\Delta\lambda. \tag{39}$$

Assuming that the coefficient of proportionality A in equation (27) for each material of the compound lens is the same (which is an acceptable assumption) and using (32), (33) and the approximation $1-\cos\varphi\approx r^2/(2f^2)$ we obtain

$$\Delta\tau(r)=\sum_1^k \frac{\lambda d_i}{c}\frac{\mathrm{d}^2 n_i}{\mathrm{d}\lambda^2}\frac{\lambda}{2N}-\frac{A}{2}\frac{\lambda}{Nc}\frac{r^2}{2f^2}\frac{\mathrm{d}f}{\mathrm{d}\lambda}. \tag{40}$$

The radius dependent part of the broadening defined as $\Delta\tau^*(r)\equiv\Delta\tau(r)-\Delta\tau(r=r_0)$ can be expressed by

$$\Delta\tau^*(r)=\frac{A}{2}\frac{\lambda}{Nc}\frac{r_0^2-r^2}{2f^2}\frac{\mathrm{d}f}{\mathrm{d}\lambda}. \tag{41}$$

From (41) and (36) it can be shown that (26) is valid in this case in the form of

$$\frac{\Delta\tau^*(r)}{\Delta T(r)}=\frac{A}{2N}. \tag{42}$$

The expression for $\Delta\tau^*(r)$ will be very complicated for the case when the coefficients A for the materials constituting the lens are not equal.

8. Propagation through a telescope

In telescopes the propagation time also depends on the input radius r. Using (9) for both lenses the delay between the phase and pulse front $\Delta T(r_2)$ is obtained as

$$\Delta T(r_2)=\frac{r_{02}^2-r_2^2}{2cf_2(n-1)}\left(-\lambda\frac{\mathrm{d}n}{\mathrm{d}\lambda}\right)\left(1+\frac{1}{M}\right). \tag{43}$$

Here $M=f_2/f_1$ is the magnification factor of the telescope. For the derivation of (43) it was assumed that the lenses both were made from the same material.

The delay can also be described by the curvature of the pulse front R (see figure 6) which can be calculated as

$$R=f_2(n-1)\left(1+\frac{1}{M}\right)^{-1}\left(-\lambda\frac{\mathrm{d}n}{\mathrm{d}\lambda}\right)^{-1}. \tag{44}$$

In (43) and (44), M is positive for a Keplerian and negative for a Galilean telescope, respectively. Thus, for a Galilean telescope the delay is smaller than for a Keplerian type.

The radius of curvature of the pulse front can also be expressed using the longitudinal chromatic aberration

$$R=\frac{f_2^2}{\lambda}\left(\frac{\mathrm{d}f_1}{\mathrm{d}\lambda}+\frac{\mathrm{d}f_2}{\mathrm{d}\lambda}\right)^{-1}. \tag{45}$$

Equation (45) is a more general expression than (44) because it is valid for telescopes in which the lenses are made from materials having different dispersions $\mathrm{d}n/\mathrm{d}\lambda$ or if

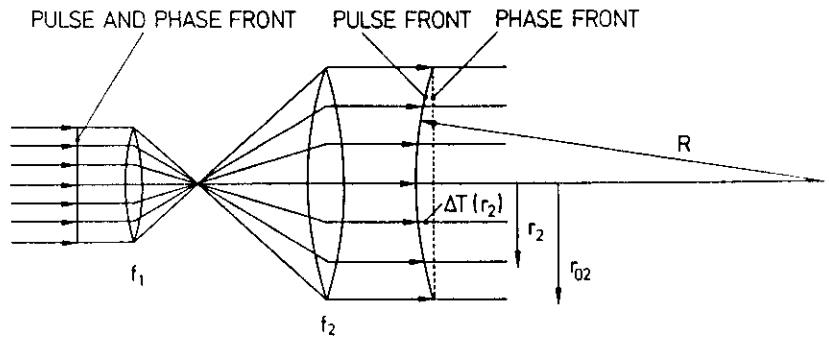

Figure 6. The phase front is flat while the pulse front has a radius of curvature of R after passing a telescope.

the lenses are compound lenses, such as nearly compensated achromats, spherically corrected doublets etc. From (45) we see that an achromatic telescope (i.e. one for which $\mathrm{d}(f_1+f_2)/\mathrm{d}\lambda=0$) introduces no pulse front distortion.

9. Conclusions

Owing to the difference between phase and group velocity, the pulse front is delayed with respect to the phase front (figure 1). For lenses this delay is a quadratic function of the input radius r (see figure 1 and equations (9), (36)). For negative lenses the delay is negative (9) (i.e. the pulse front is advanced with respect to phase front).

The delay between the axial and marginal ray is proportional to the area of the lens (9). The delay may be several picoseconds long which may considerably affect the shape of the pulse front in the vicinity of the focus (figure 3). The effect is especially important for large aperture, short focal length lenses.

The effect is larger in the ultraviolet where the dispersion of the optical materials is higher. For example, see figure 3, where the delay between the pulse and phase front for the axial ray is 4·81 ps. For a lens made of BK7 glass, having a focal length of $f=50$ mm and a diameter of $2r_0=6$ mm at 620 nm the same corresponding delay is 13 fs (9).

Behind the focus at a distance of L given by (11) or (38) the pulse front is flat. For a negative lens, L is negative which means that the flat pulse plane is located before the focus. For achromats, the delay between the pulse and phase front is constant across the beam [figure 4 and equation (22)]. A general expression which is valid for singlet lenses, compound lenses, achromats and Fresnel-zone plate was also found (36). Here the delay is described by the longitudinal chromatic aberration of the lens instead of the constructional parameters of the lenses (radii of curvature, dispersion of the refractive indices etc.). For a chromatically overcompensated doublet (i.e. $\mathrm{d}f/\mathrm{d}\lambda<0$) the delay is negative (36).

For singlet lenses, the delay caused by PTD is typically several orders of magnitude larger than the pulse broadening due to GVD (26). Nevertheless GVD

has been often considered. However, except for a few cases [14–16] the delay caused by PTD has escaped the attention of experimenters.

For achromats, the broadening due to GVD is constant over the lens cross-section (29) and thus it can be compensated by pulse compressors.

Acknowledgments

The author is grateful to Professor F. P. Schäfer for stimulating discussions, Professor A. Müller for valuable comments and J. Jethwa for critical reading of the manuscript. This work has been supported by the German–Hungarian Exchange Program, the Gottfried-Wilhelm-Leibniz-Programm and the OTKA foundation of the Hungarian Academy of Sciences.

References

[1] Topp, M. R., and Orner, G. C., 1975, *Opt. Commun.*, **13,** 276.
[2] Martinez, O. E., Gordon, J. P., and Fort, R. L., 1984, *J. opt. Soc. Am.* A, **1,** 1003.
[3] Bor, Z., and Rácz, B., 1985, *Optics Commun.*, **54,** 165.
[4] Valdmanis, J. A., Fork, R. L., and Gordon, J. P., 1985, *Optics Lett.*, **10,** 131.
[5] Martinez, O. E., 1986, *Optics Commun.*, **59,** 229.
[6] Martinez, O. E., 1987, *IEEE J. quant. Electron.*, **23,** 1385.
[7] Kafka, J. D., and Baer, T., 1987, *Optics Lett.*, **6,** 401.
[8] Duarte, F. J., 1987, *Opt. quant. Electron.*, **19,** 223.
[9] Salin, F., and Brun, A., 1987, *J. appl. Phys.*, **61,** 4736.
[10] Valdmanis, J. A., and Ford, R. L., 1986, *IEEE J. quant. Electron.*, **22,** 112.
[11] Kühlke, D., Bonkhofer, T., and von der Linde, D., 1986, *Optics Commun.*, **59,** 208.
[12] Szatmári, S., Schäfer, F. P., Müller-Horsche, E., and Mückenheim, W., 1987, *Optics Commun.*, **63,** 305.
[13] French. P. M. W., and Taylor, J. R., 1987, *Appl. Phys. Lett.*, **50,** 1708.
[14] Ihlemann, J., Helmbold, A., and Staerk, H., 1988, *Rev. scient. Instrum.* (to be published).
[15] Staerk, H., Ihlemann, J., and Helmbold, A., 1988, *Laser Optoelektron.*, **20** (to be published).
[16] Szatmári, S., and Kühnle, G., 1988, *Optics Commun.* (to be published).
[17] Born, M., and Wolf, E., 1980, *Principles of Optics*, sixth edition (Oxford: Pergamon Press).
[18] Cohen, L. G., and Lin, C., 1977, *Appl. Optics*, **16,** 3136.
[19] Pohl, R. W., 1958, *Optik und Atomphysik* (Berlin, Göttingen, Heidelberg: Springer-Verlag).
[20] Westphal, W. H., 1950, *Physik* (Berlin, Göttigen, Heidelberg: Springer-Verlag).
[21] Ditchburn, R. W., 1976, *Light* (London, New York, San Francisco: Academic Press).
[22] Malitson, I. H., 1963, *Appl. Optics*, **2,** 1103.
[23] Malitson, I. H., 1965, *J. opt. Soc. Am.*, **55,** 1205.
[24] Schott Optisches Glas Nr. 3111 d, Catalogue of the Schott Optical Glass Inc., D-6500 Mainz, Red. Rep. Germany, 1980.
[25] Treacy, E. B., 1969, *IEEE J. quant. Electron.*, **5,** 454.
[26] Bor, Z., and Rácz, B., 1985, *Appl. Optics*, **24,** 3440.
[27] Bor, Z., (to be published).

Reprinted from Optics Letters, Vol. *14*, page 119, January 15, 1989.

Distortion of femtosecond laser pulses in lenses

Z. Bor

Max-Planck-Institut für biophysikalische Chemie, Abteilung Laserphysik, Postfach 2841, D-3400 Göttingen, Federal Republic of Germany

Received June 24, 1988; accepted November 6, 1988

Large temporal front distortion of femtosecond pulses occurs in lenses having chromatic aberration. The effect is due to the difference between the phase and group velocities. Equations describing the pulse-front delay in singlet lenses, achromats, and compound lenses are presented. The pulse-front delay is several orders of magnitude larger than the broadening caused by group-velocity dispersion in the lens material. Delays occurring in Fresnel-type zone plates are also described.

The temporal shape of an ultrashort pulse may change drastically if it is propagating through a medium with dispersion. The first derivative of the refractive index with respect to the wavelength determines the difference between the phase and group velocities. The second derivative determines the pulse broadening due to group-velocity dispersion (GVD). The propagation effects occurring on refraction on plane surfaces (e.g., in prism systems) have been studied in detail and are used successfully for intracavity and extracavity pulse compression.[1–4] However, only recently has attention been paid to the propagation effects occurring in lenses and lens systems.[5–8]

In this Letter the temporal and spatial distortion of a pulse front is described on traversing a lens or lens system. The distortion is closely related to chromatic aberration of the lenses.

Owing to the difference between the phase and group velocities, the pulse front—which is defined as the surface coinciding with the peak of a pulse—is delayed with respect to the phase front. This delay can be calculated as[3,9,10]

$$\Delta T(r) = \frac{l}{c}\left(-\lambda \frac{dn}{d\lambda}\right), \tag{1}$$

where l is the path length of light in the medium having a refractive index of $n(\lambda)$.

In the range of transparency for the optical materials of practical interest, the typical value of $-\lambda(dn/d\lambda)$ is approximately 2–20%.[11] (Higher values correspond to the shorter wavelength toward the spectral cutoff.) This means that the pulse front is spatially delayed with respect to the phase front by 2–20% of the distance traveled in the medium. For femtosecond pulses such large delays cannot be neglected.

Temporal delay between the phase and pulse fronts also occurs in a lens when an ultrashort pulse traverses it. For example, a lens made from fused silica having a diameter of 80 mm and a focal length of $f = 150$ mm has a center thickness of $D = 10.5$ mm. The dispersion of silica at the wavelength of the KrF excimer laser (249 nm) is $\lambda(dn/d\lambda) = -0.1375$.[7,12] This means that for the axial ray the pulse front is delayed by 4.81 psec [see Eq. (1)], while for the marginal ray for which the distance traveled in silica is zero no delay is encountered. From the above numerical example it is obvious that the pulse front may be drastically distorted and that a detector located at the focal plane of a lens perceives a considerably longer pulse.

By using Fermat's principle and applying analytical ray tracing in the paraxial approximation, it can be shown that the delay between the phase and pulse fronts can be calculated as

$$\Delta T(r) = \frac{r_0^2 - r^2}{2cf(n-1)}\left(-\lambda \frac{dn}{d\lambda}\right), \tag{2}$$

where r and r_0 are the input paraxial radii of an arbitrary and the marginal ray, respectively (Fig. 1). The above effect is proportional to $dn/d\lambda$ and is referred to as the propagation time difference (PTD). In Eq. (2) the delay for the marginal ray (i.e., $r = r_0$) is assumed to be zero.

Behind the focus of the lens, the pulse front is changing its shape from convex to concave (Fig. 1). It can be shown that at a distance of

$$L = \frac{f}{n-1}\left(-\lambda \frac{dn}{d\lambda}\right) \tag{3}$$

the pulse front is flat, while the phase front has a radius of curvature of L. This plane is a preferred plane and in certain experiments can be used to cir-

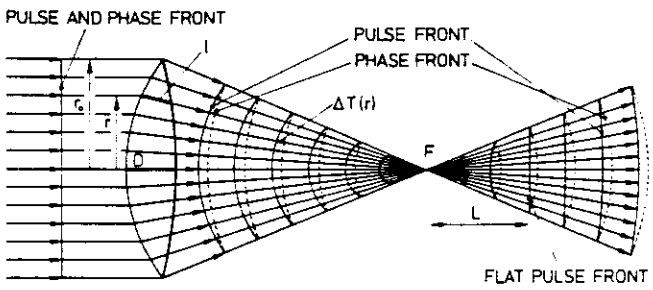

Fig. 1. Owing to the difference between the group and phase velocities, the pulse front is delayed with respect to the phase front. The delay is constant along one ray. At a distance L behind the focus the pulse front is flat.

0146-9592/89/020119-03$2.00/0

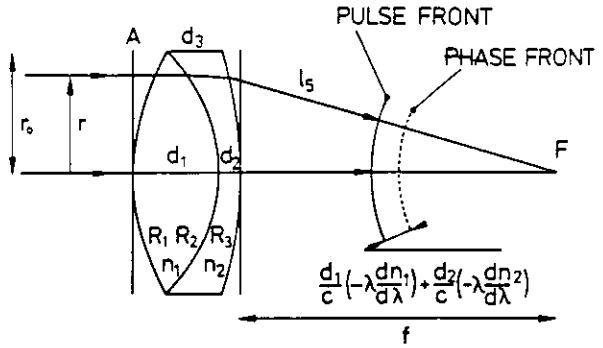

Fig. 2. For an achromat the delay between the pulse and phase fronts is constant over the cross section of the lens.

cumvent the unwanted effect of pulse-front distortion. For fused silica at 249 nm, this plane is located at $L = 0.27f$ behind the focus. (Note that the quantity L/f depends only on the material of the lens.)

Calculations show[7] that for an achromatic doublet the propagation time from plane A to the focal point F is

$$T(r) = \frac{d_1}{c}\left(n_1 - \lambda\frac{dn_1}{d\lambda}\right) + \frac{d_2}{c}\left(n_2 - \lambda\frac{dn_2}{d\lambda}\right) + \frac{f}{c}, \quad (4)$$

where the relations among the symbols are shown in Fig. 2. In the derivation of Eq. (4), Fermat's principle and the condition of achromatism obtained from $df/d\lambda = 0$ were used.[7] Thus, for an achromat, in contrast to singlet lenses, the propagation time is the same for any input radius r [Eq. (4)]. By using the condition of achromatism, it can be shown[7] that $T(r)$ can be expressed also as $T(r) = d_3/c(n_2 - \lambda dn_2/d\lambda) + f/c$.

Next we calculate the pulse broadening due to GVD. For a singlet lens the broadening of the pulse due to GVD can be calculated as[7,10]

$$\Delta\tau(r) = \frac{\lambda}{c}\frac{d^2n}{d\lambda^2}\Delta\lambda l(r), \quad (5)$$

where $l(r)$ is the path length of a ray in the lens material (Fig. 1).

It is convenient to express the bandwidth of the pulse as $\Delta\lambda = \lambda/(2N)$, where N is the number of coherent optical cycles in the pulse. (For a transform-limited pulse, where the form factor does not differ greatly from unity, $N = c\tau/\lambda$.)

A detector or a target located at the focal plane perceives both the PTD [Eq. (2)] and pulse broadening due to GVD [Eq. (5)]. Therefore, it is instructive to express their ratio from Eqs. (1) and (5) as

$$\frac{\Delta T(r)}{\Delta\tau(r)} = \frac{2}{A}N, \quad (6)$$

where A is a quantity expressing the proportionality between the second and first derivative of the refractive index.[11] A is slightly wavelength dependent and has a typical value between 2.6 and 4.0. (Higher values of A correspond to a shorter wavelength toward the spectral cutoff.[11]) Using the polynomial given for the refractive index of fused silica, we calculate that at 249 nm, $A = 3.775$.[7,12] From Eq. (6) we calculate that for a 100-fsec-long pulse for a fused-silica lens at 249 nm the exact value of the PTD is 64 times larger than broadening due to GVD.

For a singlet lens one can in general assume that for any input radius r the effect of delay between the pulse and phase fronts is approximately N times larger than the broadening of the pulse due to GVD of the lens material. The above approximation is correct with the precision of a factor of $2/A$.

For an achromat the pulse broadening due to GVD observed in the focal plane can be calculated as

$$\Delta\tau = \frac{dT(r)}{d\lambda}\Delta\lambda, \quad (7)$$

where $T(r)$ is given by Eq. (4). Taking the derivative of Eq. (4) with respect to λ, we obtain

$$\Delta\tau(r) = \frac{\lambda^2}{2cN}\left(d_1\frac{d^2n_1}{d\lambda^2} + d_2\frac{d^2n_2}{d\lambda^2}\right). \quad (8)$$

Thus for an achromat the broadening of the pulse due to GVD is independent of the input radius r. Therefore, it can be compensated for by grating[13] or prism compressors.[1-4]

In Ref. 7 a more general expression for the delay between the phase and pulse fronts has been derived:

$$\Delta T(r) = \frac{r_0^2 - r^2}{2cf^2}\lambda\frac{df}{d\lambda}, \quad (9)$$

where $df/d\lambda$ is the longitudinal chromatic aberration of the lens. Equation (9) may be useful for the calculation of the PTD because the longitudinal chromatic aberration is usually specified by the suppliers of lenses. In the paraxial approximation, Eq. (9) is valid for singlet lenses, achromatic doublets, not fully compensated achromats, and, as shown below, Fresnel-type focusing zone plates.

A zone plate (Fig. 3) for which the radii of the zones are given by

$$\rho_i = \rho_1\sqrt{i} \quad (10)$$

has a first-order focal length[14] of

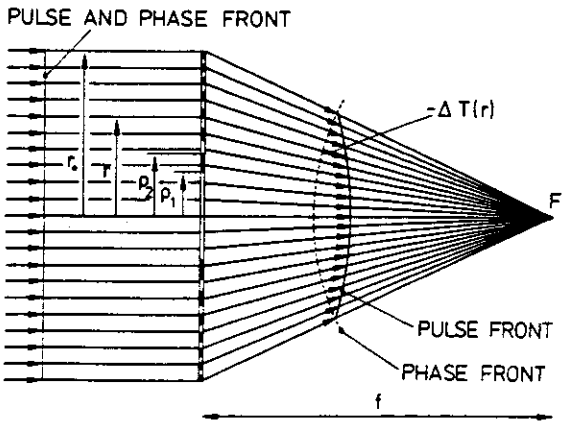

Fig. 3. For a focusing zone plate the pulse front is ahead of the phase front. The delay can be calculated using Eq. (9), obtained for refractive lenses.

$$f = \rho_1^2/\lambda. \tag{11}$$

In the paraxial approximation (i.e., $r_0/f \ll 1$; see Fig. 3) the delay between the pulse and phase fronts can be obtained after some trigonometry,

$$\Delta T(r) = -\frac{r_0^2 - r^2}{2fc}. \tag{12}$$

The negative sign in Eq. (12) expresses that the pulse front is ahead of the phase front (Fig. 3) and, as in Eq. (2), the delay for the marginal ray is regarded to be zero.

Taking the derivative of Eq. (11) with respect to λ, we obtain the longitudinal chromatic aberration of the zone plate,

$$\frac{df}{d\lambda} = -\frac{f}{\lambda}. \tag{13}$$

Combining Eqs. (12) and (13), we obtain the same expression as that obtained for a usual refractive lens [Eq. (9)].

It is surprising that Eq. (9) is also valid for a Fresnel-type focusing zone plate in which the delay between the pulse and phase fronts has a different origin compared with that of a usual refractive lens. This is a hint that Eq. (9) has a more fundamental physical meaning. It can be shown[15] that the general expression [Eq. (9)] is the manifestation of the uncertainty principle for a spectrograph consisting of a lens with chromatic aberration and a pinhole in the focus of the lens.

In conclusion, the most important properties of the pulse-front distortion occurring in lenses are summarized below:

(1) Owing to the difference between the phase and group velocities, the pulse front is delayed with respect to the phase front (Fig. 1). The delay is a parabolic function of the input beam radius [see Eq. (2)].

(2) For positive lenses, the pulse front is flat at a distance L behind the focal plane given by Eq. (3). For negative lenses this plane is before the focal plane.

(3) For singlet lenses the pulse broadening caused by GVD is in practice several orders of magnitude smaller than the delay due to the difference between the phase and group velocities [see Eq. (6)].

(4) The general equation expressing the delay through the longitudinal chromatic aberration [Eq. (9)] is valid for a Fresnel-type focusing zone plate as well.

(5) Achromats have the valuable property that the delay between the pulse and phase fronts is constant over the lens cross section [see Eq. (4) and Fig. 2]. In most experiments, this is equivalent to no delay between the two fronts. Thus, the application of achromats for most experiments can eliminate the unwanted effects of pulse-front distortion.

(6) For achromats, the pulse broadening caused by GVD is larger than for singlet lenses. However, it is constant over the cross section of the lens [see Eq. (8)]. Such spatially homogeneous pulse broadening can be compensated for by pulse compressors.

The consideration of effects listed above are particularly important in designing large-aperture, high-F-number UV optics for inertial confinement fusion experiments and x-ray laser pumping.

The author is grateful to F. P. Schäfer for stimulating discussions and J. Jethwa for critical reading of the manuscript. This research has been supported by the German–Hungarian Exchange Program and the Országos Tudományos Kutatási Alap Foundation of the Hungarian Academy of Sciences.

The author's permanent address is Research Group on Laser Physics of the Hungarian Academy of Sciences, Dóm tér 9, H-6720 Szeged, Hungary.

References

1. O. E. Martinez, J. P. Gordon, and R. L. Fork, J. Opt. Soc. Am. A **1**, 1003 (1984).
2. R. L. Fork, O. E. Martinez, and J. P. Gordon, Opt. Lett. **9**, 159 (1984).
3. Z. Bor and B. Rácz, Opt. Commun. **54**, 165 (1985).
4. J. D. Kafka and T. Baer, Opt. Lett. **6**, 401 (1987).
5. J. Ihlemann, A. Helmbold, and H. Staerk, "Chromatic time lag in picosecond-streak-camera objectives," Rev. Sci. Instrum. (to be published).
6. H. Staerk, J. Ihlemann, and A. Helmbold, Laser Optoelektron. **20**, 6 (1988).
7. Z. Bor, "Distortion of femtosecond laser pulses in lenses and lens systems," J. Mod. Opt. (to be published).
8. S. Szatmári and G. Kühnle, "Pulse front and pulse duration distortion in refractive optics, and its compensation," Opt. Commun. (to be published).
9. M. R. Topp and G. C. Orner, Opt. Commun. **13**, 276 (1975).
10. L. G. Cohen and C. Lin, Appl. Opt. **16**, 3136 (1977).
11. Z. Bor and B. Rácz, Appl. Opt. **24**, 3440 (1985).
12. I. H. Malitson, J. Opt. Soc. Am. **55**, 1205 (1965).
13. E. B. Treacy, IEEE J. Quantum Electron. **QE-5**, 454 (1969).
14. R. W. Ditchburn, *Light* (Academic, New York, 1976).
15. Z. Bor, Am. J. Phys. (to be published).

Femtosecond-resolution pulse-front distortion measurement by time-of-flight interferometry

Zsolt Bor

Research Group on Laser Physics of the Hungarian Academy of Sciences, Dom ter 9, H-6720 Szeged, Hungary

Zoltan Gogolak and Gabor Szabo

Department of Physics, Jozsef Attila University, Dom ter 9, H-6720 Szeged, Hungary

Received February 13, 1989; accepted May 23, 1989

The pulse-front distortion occurring in lenses and lens systems has been measured by a Michelson interferometer. In this technique the plane pulse front from one arm of the interferometer is used as a temporal reference level to map contour lines of equal propagation time on the pulse-front surface. The experimental arrangement is capable of detecting pulse-front distortion with a resolution of 20 fsec, and this can be improved to approximately 1 fsec. The measured value of pulse-front distortion in a telescope (1.1 psec) is in good agreement with the calculated data.

It has been shown[1-8] that certain sections of the pulse front may be delayed with respect to the phase front by several picoseconds when it traverses optical components such as prisms, lenses, and lens systems. This delay is created according to the following mechanism. The pulse front, which is defined as the surface coinciding with the peak of the pulse, moves with group velocity, while the phase front moves with phase velocity. In all materials of practical interest the group velocity is less than the phase velocity. Thus the pulse front is delayed with respect to the phase front. This delay is proportional to the dispersion $dn/d\lambda$ of the material and to the path length of the pulse in the medium.

For a positive lens the ray propagating along the optical axis has the longest path length in glass. Therefore the central part of the pulse front suffers the largest delay. For the marginal ray the path length in glass is zero, therefore no delay between the pulse front and the phase front occurs. This effect was recently described[4-6] in detail. A diagram of the pulse fronts showing how the plane input pulse front is bent after it passes twice through the telescope is shown in Fig. 1.

The equation of the spatial shape of the pulse front traversing the telescope twice (see the inset of Fig. 1) is

$$\Delta t(r) = \frac{-\lambda \frac{dn}{d\lambda}}{c f_1 (n-1)} \left(1 + \frac{f_2}{f_1}\right) r^2, \qquad (1)$$

where f_1 and f_2 are the focal lengths of the lenses, $dn/d\lambda$ is the dispersion of the lens material, and r is the input radius of an arbitrary ray. The input radius r (see Fig. 1) is defined as the distance of an arbitrary ray from the optical axis. Equation (1) is valid in the thin-lens approximation and was derived using Eq. (43) of Ref. 4 or Eq. (9) of Ref. 5. As we can see, the shape of the pulse front is a paraboloid of revolution.

In this Letter our aim is to measure the pulse-front distortion of a telescope. Such distortion can be analyzed by measuring the propagation time of a short light pulse through the optical system for different values of r, i.e., at different positions of the aperture. The Michelson interferometer can be used to measure the propagation time through the optical components. This property has been used to measure the dispersion characteristics of optical fibers[9] and to measure the optical group delay of dielectric mirrors and four-prism pulse compressors.[10] This technique resembles the time-of-flight interferometry proposed by Abramson.[11]

The interferometer used in our experiments is shown in Fig. 1. The reference arm of the interferometer is empty, thus no pulse-front distortion occurs. This means that the pulse front is a plane. The object arm contains the telescope to be studied. If the direc-

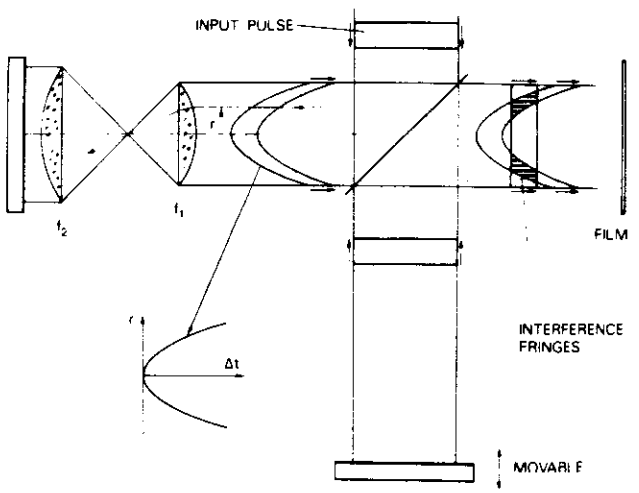

Fig. 1. Interferometer used for mapping the pulse-front distortion. Interference fringes are formed only where there is temporal and spatial overlap of the pulses coming from the reference and object arms.

0146-9592/89/160862-03$2.00/0

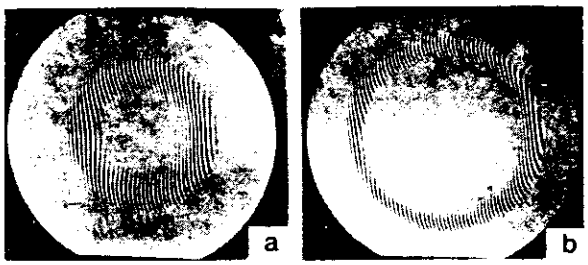

Fig. 2. Interference fringes observed at two different lengths of the reference arm. The interference fringes are formed only at those parts of the aperture where the propagation time difference between the object and reference arms does not exceed the coherence time of the illuminating beam. a, Arm shift: 0.072 mm; b, arm shift: 0.159 mm.

tion of the two beams originating from the two arms is tilted by a small angle (~0.1–0.2 mrad), then interference fringes are formed at the output.

The interference pattern is recorded photographically. The visibility of the interference fringes depends on the temporal overlap of the pulses. The fringes have unit visibility where the two temporal fronts exactly coincide, while they are gradually smeared out with decreasing overlap of the pulses. Thus the plane pulse front from one arm can be regarded as a reference level to map the contour lines of equal propagation time of the pulse-front surface from the object arm. The position of the reference level can be controlled by changing the length of the reference arm.

In the present experiments only the shift of the reference arm was measured. Thus the pulse-front delay in the telescope was measured with an uncertainty of an additive (positive or negative) constant delay. The delay was arbitrarily chosen to be zero at $r = 0$.

As discussed by Knox *et al.*[10] and Abramson,[11] instead of a short pulse a light source with a short coherence time may also be used. In our experiments a N_2-laser-pumped broadband dye laser operating at 416 nm and having a bandwidth of approximately 6 nm was used. This corresponds to an approximately 100-fsec-long coherence time.

The interferometer measures the propagation time difference in the two arms of the interferometers, therefore it is rather insensitive to the divergence of the illuminating beam. In our experiments the divergence of the dye-laser beam was 2 mrad, which was decreased by a beam expander having a magnification factor of 30. Under these conditions no effect of the divergence on the accuracy of the measurement was observed.

Figure 2 shows the interference pattern for two different lengths of the reference arm when a telescope was inserted into the object arm. Since the telescope introduces a parabolic pulse-front deformation [Eq. (1)], interference fringes are formed only in a ring-shaped area. The width of this area is determined by the coherence time of the dye laser and by the parameters of the delay parabola [Eq. (1)].

The validity of Eq. (1) was confirmed by measuring the radius of the ring, where the visibility of the fringes was the highest. This measurement was carried out as a function of Δt. The latter was changed by shifting the mirror in the reference arm. The solid line in Fig. 3 was plotted using Eq. (1). For the calculation the following parameters corresponding to our experimental conditions were used: test wavelength of $\lambda = 416$ nm, refractive index of the lens material (Schott glass K5) of $n = 1.5358$, and dispersion of Schott glass K5 at 416 nm of $dn/d\lambda = -1.3113 \times 10^{-4}$ nm^{-1}. These data were obtained from the refractive-index polynomial given by the manufacturer of the glass.[12] The focal lengths of the lenses (Spindler & Hoyer nos. 063045 and 031275) at 416 nm were $f_1 = 58.5$ mm and $f_2 = 585$ mm.

Figure 3 shows that the experimental results agree well with Eq. (1), i.e., the results of Refs. 4 and 5 can be considered to be experimentally confirmed. The scatter of the measured data is mainly caused by the uncertainty in determining the center of the rings (see Fig. 2). This uncertainty in terms of delay time is approximately 20 fsec, with the light source used having a linewidth of 6 nm.

Measurements similar to those in Fig. 3 have also been carried out at other wavelengths (455 and 501 nm). They also showed good agreement with Eq. (1).

Figure 3 also shows that the pulse-front distortion across the aperture of a lens system may be as large as 1 psec. This may drastically influence the power deposition onto a target when using femtosecond pulses.

Equation (1) describes the pulse-front distortion caused only by the difference between the group and phase velocities. However, the interferometer can

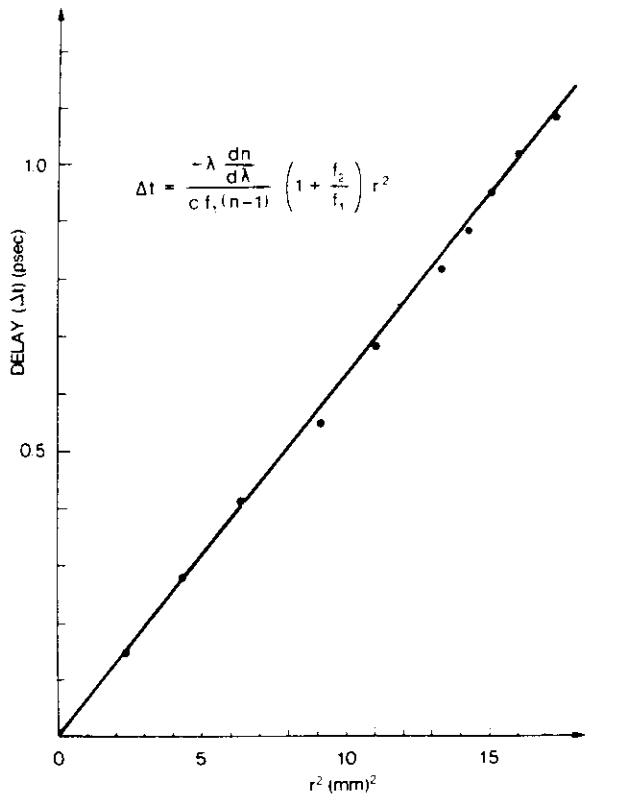

Fig. 3. Verification of Eq. (1). The pulse-front distortion is a parabolic function of the input radius.

also be used to measure the phase-front and pulse-front distortion caused by the spherical aberrations of the lenses of the telescope. In this case the dye-laser linewidth used for illuminating the telescope was narrowed to have a coherence time of approximately 10 psec, and the mirror of the reference arm was adjusted to make the output beams parallel. In this case interference fringes having a circular symmetry, which indicates spherical aberration, were observed. The number of interference fringes in this case is equal to the temporal front delay caused by spherical aberration measured in units of the optical period of the light. In our telescope the pulse-front delay caused by spherical aberrations was negligible with respect to the pulse-front delay caused by the difference between the phase and the group velocity of light.

The temporal front delay occurring in prisms was also measured with the time-of-flight technique by replacing the beam expander by a silica prism (Fig. 1). Equation (8) of Ref. 1, which describes the tilt angle between the pulse and phase fronts, was found to be correct within the accuracy of the measurements (2%).

In conclusion, the time-of-flight interferometry has been used for mapping the pulse-front distortion occurring in a beam expander. In the present experiment the temporal resolution was limited by the coherence time of the dye laser used as the light source. Using a white-light point source such as the one used by Knox *et al.*,[10] resolution as short as 1 fsec seems to be feasible. In this case, however, the insertion of a compensator glass plate into the reference arm is desirable. The glass plate may be a piece of identical dispersive material (here Schott glass K5) with a thickness equal to the axial thickness of the lens system. In addition, for short pulses pulse broadening owing to group-velocity dispersion also occurs. This effect was negligible in our present experiments; however, for pulses with a duration of only a few femtoseconds such pulse broadening might be comparable to pulse-front delay [see Eq. (27) of Ref. 4 and Eq. (6) of Ref. 5].

The time-of-flight interferometry can be used to measure the pulse-front distortion of optical components important for femtosecond spectroscopy (e.g., lenses, beam expanders, focusing optics of the targets, prisms, diffraction gratings, pulse compressors based on prisms or gratings, and Gires–Tournois interferometers). The technique can also be used to measure the pulse-front delay occurring in a single lens by forming a telescope from the lens to be studied and a spherical mirror.

This research has been supported by the Orszagos Tudomanyos Kutatasi Alap Foundation of the Hungarian Academy of Sciences and the German–Hungarian Exchange Program. The authors thank G. Kovacs for constructing the nitrogen laser and the reviewers for their valuable comments.

References

1. Z. Bor and B. Racz, Opt. Commun. **54,** 165 (1985).
2. O. E. Martinez, J. P. Gordon, and R. L. Fork, J. Opt. Soc. Am. A **1,** 1003 (1984).
3. M. R. Topp and G. C. Orner, Opt. Commun. **13,** 276 (1975).
4. Z. Bor, J. Mod. Opt. **35,** 1907 (1988).
5. Z. Bor, Opt. Lett. **14,** 119 (1989).
6. S. Szatmari and G. Kühnle, Opt. Commun. **69,** 60 (1988).
7. J. Ihlemann, A. Helmbold, and H. Staerk, Rev. Sci. Instrum. **59,** 2502 (1988).
8. H. Staerk, J. Ihlemann, and A. Helmbold, Laser Optoelektron. **20,** 34 (1988).
9. L. G. Cohen and J. Stone, Electron. Lett. **18,** 564 (1982).
10. W. H. Knox, N. M. Pearson, K. D. Li, and C. A. Hirliman, Opt. Lett. **13,** 574 (1988).
11. N. Abramson, Appl. Opt. **22,** 215 (1983).
12. *Catalogue of Schott Optical Glass Inc.* (Mainz, Federal Republic of Germany, 1980).

Volume 78, number 2 OPTICS COMMUNICATIONS 15 August 1990

Group refractive index measurement by Michelson interferometer

Z. Bor, K. Osvay, B. Rácz [1] and G. Szabó
JATE University, Department of Optics and Quantum Electronics, H-6720, Szeged, Dóm tér 9, Hungary

Received 19 February 1990

A Michelson interferometer illuminated by a polychromatic light source was used to measure the time of flight of a light pulse (or intensity substructure) through a sample of optical material. In this way the group index of optical materials (fused silica and Schott glass F3) was measured with an accuracy of 10^{-4}. The method can be also applied for measurement of the dispersive properties of optical fibers.

1. Introduction

The absolute phase refractive index n_p relates the phase velocity v_p in matter to the vacuum light velocity c as $n_p = c/v_p$. The group refractive index n_g is $n_g = c/v_g$, where v_g is the group velocity. Here v_g is defined as the speed of propagation of the envelope of a pulse (or intensity substructure of an incoherent light source) in a medium.

The group velocity can be calculated as [1–9]

$$v_g = \mathrm{d}\omega/\mathrm{d}k\,, \tag{1}$$

where ω is the angular frequency and $k = 2\,n_p(\lambda_0)/\lambda_0$ is the wave vector in the medium.

In most of the textbooks [1–9] for the group velocity the Rayleigh relation

$$v_g = v_p - \lambda\,\mathrm{d}v_p/\mathrm{d}\lambda \tag{2}$$

is given, where λ is the wavelength in the medium.

In the optical practice instead of $v_p(\lambda)$ or $\omega(k)$ the dispersion of the phase index $n_p(\lambda_0)$ is given thus (1) and (2) can not be used directly. Therefore it is useful to rewrite (1) as [10–14]

$$v_g = \frac{\mathrm{d}\omega}{\mathrm{d}k} = \frac{\mathrm{d}\omega_0}{\mathrm{d}\lambda_0}\frac{\mathrm{d}\lambda_0}{\mathrm{d}k} = \frac{c}{n_p - \lambda_0\,\mathrm{d}n_p/\mathrm{d}\lambda_0} \tag{3}$$

[1] Research Group on Laser Physics, Hungarian Academy of Sciences, H-6720, Szeged, Dóm tér 9, Hungary.

from where

$$n_g = n_p - \lambda_0\,\mathrm{d}n_p/\mathrm{d}\lambda_0\,. \tag{4}$$

In some of the textbooks [3,5–7] for the group velocity v_g and the group refractive index n_g ambiguous expressions are given. The ambiguity comes from the confusion of the wavelength in vacuum and in the material.

The phase index n_p is usually measured using a Snell's law applied to a prism or other refractive surfaces or by measuring the critical angle of the total internal reflection [2–9,16]. The group index can be calculated from (4) using the measured values of $n_p(\lambda_0)$ [10,14,16]. Besides, n_g can also be measured directly by measuring the propagation time of short pulses over a known distance [12,13,15,17–19]. However this is rather expensive and complicated method.

In this paper we show a very simple and high precision method for measuring the group index n_g using a Michelson interferometer.

2. Polychromatic interference fringes with a Michelson interferometer

Fig. 1a shows a Michelson interferometer illuminated by a polychromatic light source. (In this paper a light source having a few nm bandwidth will be referred as polychromatic.) One of the mirrors is tilted by about 0.1 mrad. In this way on the screen a few

0030-4018/90/$03.50

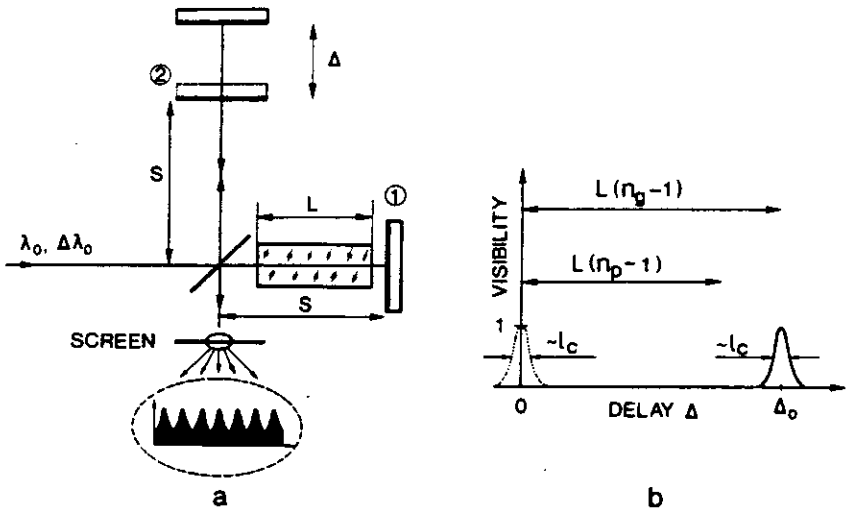

Fig. 1. (a) The Michelson interferometer is measuring the group refractive index of the sample inserted into arm 1. One of the mirrors is slightly tilted, thus interference fringes are observed on the screen. (b) The visibility of the interference fringes depends on the position Δ of mirror 2 (solid line: sample is inserted into arm 1, dotted line: without sample). The half width of the visibility curves is about the coherence length of the light source (0.06 mm).

interference fringes appear. When the arms are empty, interference fringes can be observed only in case the difference of the length Δ between the two arms is less than the coherence length l_c. The latter can be estimated as

$$l_c = \lambda_0^2/(2\delta\lambda_0) .$$

If the length of arm 2 is increasing, the visibility of the interference fringes gradually decreases to zero. The halfwidth of this curve is about l_c (see the dotted line on fig. 1b). If a parallel plate of optical material having a refractive index of $n_p(\lambda_0)$ and a length of L is inserted into arm 1 then the phase shift in this arm is

$$\varphi_1 = (4\pi/\lambda_0)\,[(S-L)+Ln_p(\lambda_0)] . \qquad (5)$$

If the length of arm 2 is increased by Δ, then the phase shift of this arm is

$$\varphi_2 = (4\pi/\lambda_0)\,[S+\Delta] . \qquad (6)$$

Interference fringes with polychromatic light can be observed if

$$(\mathrm{d}/\mathrm{d}\lambda_0)\,(\varphi_1-\varphi_2)=0 . \qquad (7)$$

By taking the derivatives of (5) and (6) we obtain that (7) is fulfilled if

$$\Delta_0 = L(n_g-1) , \qquad (8)$$

where n_g is the group index of the optical material given by (4).

Eq. (8) means that upon introduction of the glass plate into arm 1, interference fringes with visibility $V=1$ are observed only if the length of arm 2 is increased by $\Delta=\Delta_0$ (see fig. 1b). If (8) is not fulfilled, then (7) is also not fulfilled and the interference fringes formed by different wavelength components of the polychromatic light source will be spatially slightly shifted with respect to each other. If $|\Delta-\Delta_0|$ exceeds the coherence length l_c then due to such shift of the fringes the interference pattern will be smeared out.

Eq. (8) is somewhat surprising, since it means that in spite of the fact that the introduction of the material into one of the arms increases the optical path by $L(n_p-1)$, an increase of the arm length by $L(n_g-1)$ is necessary to observe polychromatic fringes (fig. 1b). However (8) is in full agreement with the physical meaning of n_g, since v_g is the speed of propagation of the envelope of the light intensity. The latter statement is valid both for short pulses and for the intensity substructure of an incoherent polychromatic radiation.

A relation similar to (8) has already been derived long ago in connection with the compensating plate of white light Michelson interferometers [23], however, the possibility to use it for direct measurement of the group refractive index has escaped the attention of later researchers.

The equations (5)–(8) are slightly changed, when the refractive index of the laboratory air is also taken into account. The phase shifts in the arms in such case will be

$$\varphi_1 = (4\pi/\lambda_0)\,[(S-L)n_p^a + Ln_p(\lambda_0)]\,, \tag{9}$$

$$\varphi_2 = (4\pi/\lambda_0)\,[(S+\Delta)n_p^a]\,, \tag{10}$$

where n_p^a is the phase refractive index of the air.

The condition (7) is fulfilled if

$$\Delta_0 = L(n_g/n_g^a - 1)\,, \tag{11}$$

where n_g is the group index of the optical material and

$$n_g^a = n_p^a - \lambda_0 \mathrm{d}n_p^a/\mathrm{d}\lambda_0 \tag{12}$$

is the group index of the air. The latter can be calculated from (4) using the refractive index (n_p^a) polynomial given for air [22]. As an example at $p=760$ Torr, $T=15$ °C, for $\lambda_0=450$ nm we calculated $n_p=1.0002795$ and $n_g=1.0002953$.

3. Experimental arrangement

Our interferometer (fig. 1a) used a beam splitter cube (Spindler and Hoyer N°33520) therefore no compensating plate [2] was necessary. The measurements have been carried out in air at room temperature.

The mirror of arm 2 was on a translator stage having a resolution of 0.001 mm. The light source used for illuminating the Michelson interferometer was a N_2-laser pumped tunable dye laser having a bandwidth of about 2 nm, which corresponds to a coherence length of about 0.06 mm. The interference fringes were observed on a screen visually. The length of arm 2 was set to have maximum visibility. The reproducibility of setting the length of arm 2 was less than ±0.01 mm. The length of the sample was measured with a comparator having an accuracy of ±0.002 mm. By measuring the value of Δ_0 the group index was calculated from (11).

4. Experimental results

Fig. 2 shows the group and phase index of fused silica (Suprasil B). The group index n_g was measured on a sample having $L=54.165$ mm length using the expression (11). For comparison the phase index measured by Malitson [20] using the minimum deviation angle method is also shown. The group index calculated from the n_p polynomial [20] using (4) are shown as well.

The agreement between the theoretical and experimental data of n_g is excellent. The error is as small as 0.95×10^{-4}. Notice, that this is about 3 times smaller than the effect of the refractive index of the laboratory air on the accuracy of the measurements (compare (8) and (11)).

We believe, that with more sophisticated mechanical components and with electronic registration of the interference fringes [17] precision approaching 10^{-5} could be achieved. This is the same as the accuracy of the minimum deviation method [20] for measuring the phase refractive index n_p.

The accuracy of the present measurements is

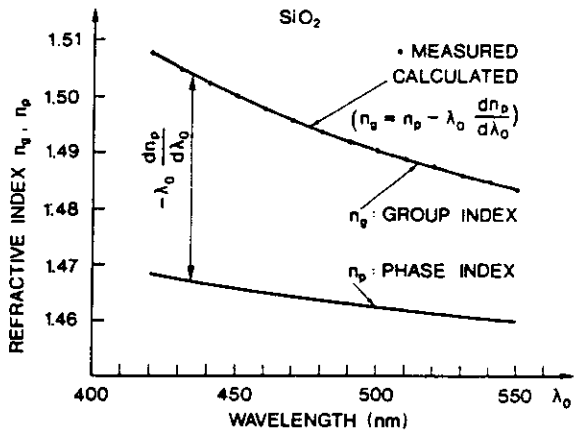

Fig. 2. Group and phase refractive index of fused silica. The group index was measured by the interferometer shown on fig. 1a. The phase index was calculated from the polynomial given by Malitson [20]. The group index was calculated from the phase index using (4). The difference (standard deviation) between calculated and measured values of the group index is 9.5×10^{-5}.

somewhat affected by the fact that the group velocity itself is also wavelength dependent. E.g. at 505 nm $dn_g/d\lambda_0 = -1.562\times10^{-4}$/nm. However this is a linear dependence, thus, it is averaged out over the 2 nm bandwidth of the measuring light. At the same wavelength $d^2n_g/d\lambda_0^2$ is about 9×10^{-7}/nm^2 which causes an error much less than the errors due to the mechanical accuracy of the interferometer. The possibility to increase the accuracy of the method below 10^{-4} is under progress.

Similar measurements of the group index was made with a piece of $L = 197.241$ mm long Schott glass F3. Here the phase refractive index was calculated from the polynomial specified in ref. [21]. The accuracy of the agreement between calculated and measured data of n_g were the same as for silica.

5. Conclusions

The insertion of an optical material into one of the arms of a Michelson interferometer increases the optical pathlength by $L(n_p-1)$. However the envelope of the intensity is delayed by $L(n_g-1)$. In this way the Michelson interferometer using a polychromatic light source measures the time of flight of a pulse (or intensity substructure) through a sample. Therefore it can be used for direct measurement of the group index. The arrangement is similar to the time-of-flight interferometer described in ref. [18]. The same principle can be used with other two beam interferometers (e.g. Jamin, Mach-Zender, Twyman-Green, etc.). The method can also be used for measuring the dispersive properties of optical fibers.

Finally we would like to emphasize that the relation (8) or (11) is valid both for monochromatic and for polychromatic light sources. However the condition to observe the difference between $L(n_p-1)$ and $L(n_g-1)$ (see fig. 1b) is that the coherence length should be much less than $L(n_g-n_p)$, i.e.

$$\lambda_0^2/2\delta\lambda_0 \ll L\lambda_0 dn_p/d\lambda_0 . \qquad (13)$$

In our case at $\lambda_0 = 500$ nm the value of $L(n_g-n_p) = 1.499$ mm, which is much larger than the coherence length ($l_c = 0.06$ mm) of our dye laser. Therefore the validity of (8) or (11) could be clearly proved. However a HeNe laser having a typical coherence length of 100 mm is not suitable for measuring the difference between n_g and n_p.

Acknowledgement

This work has been supported by the OTKA Foundation of the Hungarian Academy of Sciences.

References

[1] L. Brillouin, Wave propagation and group velocity (Academic Press, New York, London, 1960).
[2] M. Born and E. Wolf, Principles of optics (Pergamon, New York, 1975).
[3] E. Hecht and A. Zajac, Optics (Addison-Wesley, Reading, Mass. 1974).
[4] F.A. Jenkins and H.E. White, Physical optics (McGraw-Hill, London, 1976).
[5] R.W. Pohl, Optik und Atomphysik (Springer Verlag, Berlin, Göttingen, Heidelberg, 1976).
[6] R.W. Ditchburn, Light (Academic Press, London, New York, San Francisco, 1976).
[7] D.V. Sivuchin, Obshiy Kurs Physiki (Nauka, Moskow, 1985).
[8] R.S. Longhurst, Geometrical and physical optics (Longman, London, New York, 1973).
[9] L. Bergman and C. Schaefer, Optik (W. De Gruyter, Berlin, 1966).
[10] M.R. Topp and G.C. Orner, Optics Comm. 13 (1975) 276.
[11] Z. Bor and B. Rácz, Optics Comm. 54 (1985) 165.
[12] C. Lin, L. Cohen, W.G. French and H.M. Presby, IEEE J. Quantum Electron. QE-16 (1980) 33.
[13] L. Cohen and C. Lin, Appl. Optics 16 (1977) 3136.
[14] A. Brimontas, V. Vasilyauskas, A. Piskarskas and A. Stabibis, Sov. J. Quantum Electron. 15 (1985) 787.
[15] D.B. McDonald and S.A. Rice, Optics Comm. 32 (1980) 416.
[16] K. Schmidt and A. Penzkofer, Appl. Optics 22 (1983) 1824.
[17] W.H. Knox, N.M. Pearson, K.D. Li and C.A. Hirliman, Optics Lett. 13 (1988) 574.
[18] Z. Bor, Z. Gogolák and G. Szabó, Optics Lett. 14 (1989) 862.
[19] H. Staerk, J. Ihlemann and A. Helmbold, Laser und Optoelectronik 20 (1988) 34.
[20] I.H. Malitson, Appl. Optics 2 (1963) 1103.
[21] Schott Optisches Glass Nr. 3111 d (Catalogue of the Schott Optical Glass Inc., Mainz, Fed. Rep. Germany, 1980).
[22] Handbook of Chemistry and Physics (Chemical Rubber Co., Cleveland, Ohio, 1970).
[23] E.C. Craven, Proc. Phys. Soc. 57 (1945) 97.